The role of the key effector of necroptotic cell death, MLKL, in mouse models of disease

Tovey Crutchfield E. [1,2,3]; Garnish S.E[2,3]. and Hildebrand J.M[2,3,^].

[1] Department of Medical Education, University of Melbourne; Parkville, VIC 3052, Australia

[2] The Walter and Eliza Hall Institute of Medical Research, Parkville, VIC 3052, Australia

[3] Department of Medical Biology; University of Melbourne; Parkville, VIC 3052, Australia

^ To whom correspondence may be addressed; jhildebrand@wehi.edu.au

Abstract: Necroptosis is an inflammatory form of lytic programmed cell death that is thought to have evolved to defend against pathogens. Genetic deletion of the terminal effector protein – MLKL – shows no overt phenotype in the C57BL/6 mouse strain under conventional laboratory housing conditions. Small molecules that inhibit necroptosis by targeting the kinase activity of RIPK1, one of the main upstream conduits to MLKL activation, have shown promise in several murine models of non-infectious disease and in phase II human clinical trials. This has triggered multi-billion-dollar investments into the emerging class of necroptosis blocking drugs, and the potential utility of targeting the terminal effector is being closely scrutinised. Here we review murine models of disease, both genetic deletion and mutation, that investigate the role of MLKL. We summarize a series of examples from several broad disease categories including ischemia reperfusion injury, sterile inflammation, pathogen infection and haematological stress. Elucidating MLKL's contribution to mouse models of disease is an important first step to identify human indications that stand to benefit most from MLKL-targeted drug therapies.

Keywords: Necroptosis, MLKL, programmed cell death

 doi:10.20944/preprints202105.0053.v1

Acknowledgements: JMH is the recipient of an Australian NHMRC Career Development Fellowship 1142669. SG is the recipient of The Wendy Dowsett Scholarship. ETC is the recipient of the Attracting and Retaining Clinician-Scientists (ARCS) scholarship. We wish to thank James Murphy, Cheree Fitzgibbon and Andre Samson for their careful reading of this manuscript and helpful suggestions.

Preprints (www.preprints.org) | NOT PEER-REVIEWED | Posted: 5 May 2021 doi:10.20944/preprints202105.0053.v1

Introduction:

Necroptosis and disease.

Mixed Lineage Kinase Domain-Like (MLKL) was shown to be the essential effector of a pro-inflammatory, lytic form of programmed cell death called necroptosis in 2012 (Sun et al., 2012) (J. Zhao et al., 2012). Necroptosis is characterised by the release of Damage-associated Molecular Patterns (DAMPs) and IL-33, IL-1α and IL-1β production as recently reviewed by (Weir, Hughes, Rashidi, Hildebrand, & Vince, 2021). Unlike apoptosis, necroptosis and the canonical signalling pathway RIPK1-RIPK3-MLKL, is not essential to the development and homeostasis of multicellular organisms (Samson, Garnish, Hildebrand, & Murphy, 2021). The two most downstream effectors of necroptosis, MLKL and its obligate activating kinase RIPK3, can be deleted at the genetic level in laboratory mice without any overt developmental consequences in the absence of challenge (Murphy et al., 2013; J. Wu et al., 2013), (Newton, Sun, & Dixit, 2004). Thus, it is widely held that MLKL and necroptosis have evolved primarily to defend against pathogenic insult to cells and tissues. This important role of necroptosis in pathogen defence is written in the DNA of many bacteria and viruses alike, which together encode several genes that disarm different facets of the necroptotic signalling pathway (Silke & Hartland, 2013) (Pearson & Murphy, 2017) (Petrie et al., 2019). In evolution, genetic deletion of MLKL and/or RIPK3 in the ancestors of modern day carnivora, metatheria (marsupials) and aves (birds) show that complex vertebrates can survive without necroptosis when faced with infectious challenges of the ‘real world’ (Dondelinger, Hulpiau, Saeys, Bertrand, & Vandenabeele, 2016). This adds to the precedent for the well-honed flexibility, redundancy and co-operation of different programmed cell death pathways in the

Preprints (www.preprints.org) | NOT PEER-REVIEWED | Posted: 5 May 2021 doi:10.20944/preprints202105.0053.v1

defence against pathogens (Doerflinger et al., 2020), and offers some biological guide that inhibiting MLKL pharmacologically in humans would not compromise pathogenic defence. Interestingly, recent studies suggest that the suppression of necroptosis may even reduce the resulting inflammatory response that is often more dangerous than the infection itself (T. Zhang et al., 2020). *Mlkl*$^{-/-}$ mice are distinguishable from wild-type mice in numerous models of disease, a broad sampling of which is presented here in (Table 1).

The therapeutic potential for necroptosis-targeted drugs lies largely in non-infectious indications. The first human clinical trials of RIPK1-targetted small molecule compounds were conducted in cohorts of rheumatoid arthritis, ulcerative colitis and psoriasis patients (Sheridan, 2019). While these showed some promise in phase 2, these were returned to research phase in late 2019 by their licensee GlaxoSmithKline (GSK, 2019). At the time of writing, there are only two active clinical trials in progress; a phase I trial assessing the safety of a new RIPK1 inhibitor (GFH312) and a phase II study utilising RIPK1-binding compound, SAR443122, (licensed by Sanofi) in cutaneous lupus erythematosus patients. There are currently no 'first in human' trials of RIPK3- or MLKL- binding compounds listed on http://clinicaltrials.gov.

Mlkl Knock-Out (KO) and Constitutively Active (CA) mice at steady state.

Following the discovery of its essential role in necroptosis (J. Zhao et al., 2012) (Sun et al., 2012), two *Mlkl* knockout mouse strains were independently generated by traditional homologous recombination (Murphy et al., 2013) and TALEN technology (J. Wu et al., 2013). More recently, CRISPR-Cas9 engineered *Mlkl*$^{-/-}$ (Dannappel et al., 2014; Li et al., 2017);(Ni et al., 2019), constitutively active point mutant *Mlkl*^{D139V}

Preprints (www.preprints.org) | NOT PEER-REVIEWED | Posted: 5 May 2021 doi:10.20944/preprints202105.0053.v1

(Hildebrand et al., 2020), affinity tagged *Mlkl* (Ying et al., 2018), conditional *Mlkl*$^{-/-}$ strains (J. Lin et al., 2016) (Ying et al., 2018) and antisense oligonucleotide (ASOs) *in vivo Mlkl* knockdown (Rasheed et al., 2020) mouse models have also been used in the study of necroptosis.

Mlkl$^{-/-}$ mice are born at expected Mendelian ratios and are overtly indistinguishable from wild-type littermates at birth and through to early adulthood (Murphy et al., 2013; J. Wu et al., 2013). Full body histological examination of 2 day old *Mlkl*$^{-/-}$ pups did not reveal any obvious morphological differences, including lesions or evidence of inflammation, relative to wild-type C57BL/6 mice of the same age (Hildebrand et al., 2020). Furthermore, no histological differences have been reported for the major organs of young adult *Mlkl*$^{-/-}$ mice (Murphy et al., 2013) (J. Wu et al., 2013). Hematopoietic stem cell populations in the bone marrow (Murphy et al., 2013) and CD4/CD8 T cell, B cell, macrophage and neutrophil mature cell populations in secondary lymphoid organs display no observable differences in adult mice (Wu et al., 2013). At steady state, serum cytokines and chemokines are indistinguishable from age-matched wild-type mice (Alvarez-Diaz et al., 2016). The genetic absence of *Mlkl* and thus necroptosis, is generally considered to be innocuous at steady state in the C57BL/6 strain of laboratory mice at a typical experimental age (up to 16 weeks) that are housed under conventional clean, pathogen free conditions.

Mlkl$^{-/-}$ mice in ischemia and reperfusion injury (IRI).

While grouped here for simplicity, MLKL and cell death in general has the potential to influence many facets of the physiological response to blood vessel occlusion/recanalisation and resultant end-organ damage. These facets include the

Preprints (www.preprints.org) | NOT PEER-REVIEWED | Posted: 5 May 2021 doi:10.20944/preprints202105.0053.v1

aetiology of the infarction itself, the cellular damage incurred due to the deprivation of oxygen and ATP, the generation of reactive oxygen species that occurs following tissue reperfusion, the inflammation that ensues and convalescence after injury (Luedde, Kaplowitz, & Schwabe, 2014). As summarized in Table 1 (see 'ischemia and reperfusion injury'), *Mlkl*$^{-/-}$ mice appear partially protected from the initial embolic insult (Yang et al., 2018) (Shi et al., 2020). For example, *Mlkl*$^{-/-}$ mice were reported to exhibit reduced infarct size and have better locomotive recovery day 7 post stroke (Shi et al., 2020). This protective effect may in part be due to the role of MLKL and RIPK3 in regulating platelet function and homeostasis (Y. Zhang et al., 2017) (Moujalled et al., 2021). *Mlkl* knockout is also protective in models of hepatic and renal IRI (Müller et al., 2017)(Newton et al., 2016). Neutrophil activation and inflammation are significant contributors to hepatic IR injury (Hasegawa et al., 2007). Despite equivalent levels at steady state, the *Mlkl*$^{-/-}$ mice liver parenchyma shows significantly lower numbers of neutrophils 24 hours post infarct (Ni et al., 2019). This reinforces that the absence of MLKL can play a protective role at the initial ischaemic stage, and/or at later reperfusion stages, depending on the context.

Sterile inflammation.

The contribution of MLKL to mouse models of inflammation, which are not borne of pathogenic insult, termed sterile inflammation, is complex and varies according to the initiator, severity and location within the body. This point is nicely illustrated by systemic inflammatory response syndrome (SIRS). Unlike catalytically inactive RIPK1 or RIPK3 deficiency in mice, *Mlkl*$^{-/-}$ mice are not protected against SIRS driven by *low* dose TNFα (Newton et al., 2016) or A20 deficiency (Newton et al., 2016). When wild-type mice are pre-treated with compound 2, a potent inhibitor of necroptosis that binds

Preprints (www.preprints.org) | NOT PEER-REVIEWED | Posted: 5 May 2021 doi:10.20944/preprints202105.0053.v1

to RIPK1, RIPK3 and MLKL, they are protected from hypothermia (Pierotti et al., 2020). Together these findings suggest protection against SIRS is necroptosis-independent and occurs upstream of MLKL. *Mlkl*$^{-/-}$ mice, however, are significantly protected against SIRS caused by *high* dose TNFα (Moerke, Bleibaum, Kunzendorf, & Krautwald, 2019; Pierotti et al., 2020) (Pierotti et al., 2020) (Newton et al., 2016) or SHARPIN-deficiency (Rickard et al., 2014). *Ripk3*$^{-/-}$ mice are similarly protected against high dose TNFα. Remarkably, in contrast to single knockouts, *Ripk3*$^{-/-}$, *Mlkl*$^{-/-}$ double knockouts resemble wild type mice, but develop severe hypothermia in response to high dose TNF (Moerke et al., 2019), a paradoxical reaction that is yet to be fully explained by the field. Furthermore, the ablation of MLKL is seen to worsen inflammation induced by non-cleavable caspase-8 (seen in *Casp8*$^{D387A/D387A}$ mice) (Tummers et al., 2020) and A20 deficiency (Newton et al., 2016). This indicates that necroptosis may serve to limit systemic inflammation in certain scenarios *in vivo*, a phenomenon also supported by examples of pathogen induced inflammation (see 'Infection', Table 1).

One major area of contention is the role of MLKL in mouse models of inflammatory bowel disease (Shindo et al., 2019) (Schwarzer, Jiao, Wachsmuth, Tresch, & Pasparakis, 2020), (Alvarez-Diaz et al., 2020) (Xie Y et al., 2020 JCI) and inflammatory arthritis (Polykratis et al., 2019) (Lawlor et al., 2015); however key differences in experimental approach may explain these disparities (See Table 1, '*Mlkl*$^{-/-}$ mice and wild-type control' details). Similarly, there have been conflicting reports investigating the role of MLKL-driven necroptosis in livery injury (Hamon, Piquet-Pellorce, Dimanche-Boitrel, Samson, & Le Seyec, 2020) (Günther et al., 2016). Whilst constitute knock-out of MLKL confers protection (Günther et al., 2016), a refined method that

involves hepatocyte-specific ablation of MLKL, reveals that necroptosis in parenchymal liver cells is, in fact, dispensable in immune-mediated hepatitis (Hamon et al., 2020). It would therefore be of interest to know the cell type, in which *Mlkl*$^{-/-}$ drives protection, now that hepatocytes (Hamon et al., 2020) and immune cells (Günther et al., 2016) have been ruled out. MLKL-deficiency mediates protective effects in models of more localised sterile inflammatory disease: dermatitis (Devos et al., 2020), cerulein-induced pancreatitis (Wu et al., 2013), ANCA-driven vasculitis (Schreiber et al., 2017), necrotising crescent glomerulonephritis (Schreiber et al., 2017) and oxalate nephropathy (Mulay et al., 2016). Consistent with these findings, mice expressing a constitutively active form of MLKL develop a lethal perinatal syndrome, characterised by acute multifocal inflammation of the head, neck and mediastinum (Hildebrand et al., 2020).

Infection: bacterial.

MLKL-dependent necroptosis is thought to have evolved as a pathogen-clearing form of cell death. In support of this theory, 7 out of the 10 murine models of bacterial infection examined here led to poorer outcomes in mice lacking MLKL. In response to both acute and chronic infection with *Staphylococcus aureus* and methicillin-resistant *S. aureus* (MRSA), *Mlkl*$^{-/-}$ mice suffer a greater bacterial burden and subsequent mortality (Kitur et al., 2016) (D'Cruz et al., 2018). This was observed across intravenous, subcutaneous, intraperitoneal, and retro-orbital methods of inoculation (Kitur et al., 2016) (D'Cruz et al., 2018). Interestingly, despite necroptosis being an inflammatory form of cell death, *Mlkl*$^{-/-}$ mice were found to have greater numbers of circulating neutrophils and raised inflammatory markers (caspase 1 and IL-1β) (Kitur et al., 2016) (D'Cruz et al., 2018). This is exemplified in models of skin infection where

Preprints (www.preprints.org) | NOT PEER-REVIEWED | Posted: 5 May 2021 doi:10.20944/preprints202105.0053.v1

Mlkl$^{-/-}$ mice suffer severe skin lesions characterised by excessive inflammation (Kitur et al., 2016). This suggests that necroptosis is important for limiting bacterial dissemination and modulating the inflammatory response (Kitur et al., 2016). As an example, MLKL-dependent neutrophil extracellular trap (NET) formation was reported to restrict bacterial replication (D'Cruz et al., 2018) and contribute to the pathogenesis of inflammatory disease, such as rheumatoid arthritis (Khandpur et al., 2013). In addition to the important infection-busting role of MLKL in neutrophils, non-haematopoietic MLKL is also important for protection against gut-born infections. MLKL-mediated enterocyte turnover and inflammasome activation were shown to limit early mucosal colonisation by Salmonella (Yu et al., 2018). MLKL was even shown to bind and inhibit the intracellular replication of Listeria, presaging exploration into a more direct, cell-death independent mode of MLKL-mediated pathogen defence (Sai, Parsons, House, Kathariou, & Ninomiya-Tsuji, 2019).

Through co-evolution, bacteria have developed ways to evade, and in some cases, weaponise MLKL and necroptosis for their own end. Certain bacteria, such as *Serratia marcescens* and *Streptococcus pneumoniae* produce pore-forming toxins (PFTs) to induce necroptosis in macrophages and lung epithelial cells (González-Juarbe et al., 2015) (Gonzalez-Juarbe et al., 2020). *Mlkl*$^{-/-}$ mice are consequently resistant to these infections and survive longer than wild-type controls (González-Juarbe et al., 2015; Gonzalez-Juarbe et al., 2020). Although PFT-induced necroptosis was reported to exacerbate pulmonary injury in acute infection, it does promote adaptive immunity against colonising pneumococci (Riegler, Brissac, Gonzalez-Juarbe, & Orihuela, 2019). *Mlkl*$^{-/-}$ mice demonstrate a diminished immune response, producing less anti-*spn* IgG antibody and thus succumb more readily to secondary lethal *S. pneumoniae*

Preprints (www.preprints.org) | NOT PEER-REVIEWED | Posted: 5 May 2021 doi:10.20944/preprints202105.0053.v1

infection (Riegler et al., 2019). This suggests necroptosis is instrumental in the natural development of immunity to opportunistic PFT- forming bacteria (Riegler et al., 2019). This is of significance as 80 serotypes of *S. pneumoniae* are currently not covered in the adult vaccine (Prevention, 2019). Of note, *Mlkl*$^{-/-}$ mice are indistinguishable from wild-type controls in CLP-induced polymicrobial shock (J. Wu et al., 2013) and subsequent acute kidney injury (Sureshbabu et al., 2018). Results derived from the CLP model of shock can be hard to replicate, given the inter-facility and even, intra-facility, heterogeneity of the cecal microbiota in mice (Wu et al., 2013). Cell death pathways occur simultaneously during the progression of sepsis and there is no conclusive evidence of which pathway plays the most deleterious role (Wu et al., 2013). Similarly, MLKL appears dispensable for granulomatous inflammation and restriction of *Mycobacterium tuberculosis* colonisation (Stutz et al., 2018).

Infection: Viral

MLKL can either protect against viral infection or contribute to viral propagation and/morbidity, depending on the type of virus. In initial studies, *Mlkl*$^{-/-}$ mice were indistinguishable from wild-type littermates in response influenza A (IAV) (Nogusa et al., 2016) (T. Zhang et al., 2020) (Shubina et al., 2020) and West Nile virus infection (Daniels et al., 2017). Recent findings, however, suggest that *Mlkl* knockout confers protection against lung damage from lethal doses of influenza A (T. Zhang et al., 2020). Despite equivalent pulmonary viral titres to wild-type littermates, *Mlkl*$^{-/-}$ mice had a considerable attenuation in the degree of neutrophil infiltration (~50%) and subsequent NET formation and thus, were protected from the exaggerated inflammatory response that occurs later in the infection (T. Zhang et al., 2020). In line with this finding, *Mlkl*$^{-/-}$ mice are protected against bacterial infection secondary to IAV

Preprints (www.preprints.org) | NOT PEER-REVIEWED | Posted: 5 May 2021 doi:10.20944/preprints202105.0053.v1

(Gonzalez-Juarbe et al., 2020). A recent study also finds that MLKL-deficiency mediates protection against cardiac remodelling during convalescence following IAV infection by upregulating antioxidant activity and mitochondrial function (Y. H. Lin et al., 2021), indicating the potential utility of MLKL-targeted therapies for both the acute and long term effects of viral infection.

Metabolic disease.

We examine four models of non-alcoholic fatty liver disease (NAFLD) where MLKL deficiency has shown diverse effects. 18 hours after choline-deficient methionine-supplemented diet (Tsurusaki et al., 2019) or after 8 weeks of a Western-diet (Ni et al., 2019), *Mlkl*$^{-/-}$ mice are indistinguishable from wild-type controls. Following 12 weeks of a high fat diet (Saeed et al., 2019), however, *Mlkl*$^{-/-}$ mice appear resistant to steatohepatitis given that MLKL-deficiency promotes reduced *de novo* fat synthesis and chemokine ligand expression (Saeed et al., 2019). A similar effect is seen following 12 weeks of a high fat, fructose and cholesterol diet where *Mlkl*$^{-/-}$ mice are markedly protected against liver injury, hepatic inflammation and apoptosis attributed to inhibition of hepatic autophagy (X. Wu et al., 2020). MLKL does not appear to play a statistically significant role in acute or chronic alcoholic induced fatty liver disease (Miyata et al., 2021).

MLKL deficiency provides variable protection against the metabolic syndrome, depending on the challenge. MLKL deficiency appears to protect against dyslipidaemia; reduced serum triglyceride and cholesterol levels following a high fat

Preprints (www.preprints.org) | NOT PEER-REVIEWED | Posted: 5 May 2021 doi:10.20944/preprints202105.0053.v1

diet (Saeed et al., 2019) and Western diet (Rasheed et al., 2020) respectively. Whilst *Mlkl*$^{-/-}$ mice appear to have significantly improved fasting blood glucose levels following 16 weeks of a high fat diet (H. Xu et al., 2019) there is conflicting evidence on the effect at steady state (H. Xu et al., 2019) (Saeed et al., 2019). There is also conflicting evidence on the role of MLKL deficiency in adipose tissue deposition and weight gain (Saeed et al., 2019) (H. Xu et al., 2019). Finally, MLKL has been shown to play a role in atherogenesis; MLKL facilitates lipid handling in macrophages and upon inhibition, size of the necrotic core in the plaque is reduced (Rasheed et al., 2020). Of the eight broad disease classes covered in this review, the role of MLKL in metabolic disease is arguably the most disputed owing to the long-term nature of the experiments and the propensity for confounding variables including genetic background and inter-facility variation in microbiome composition. The field may benefit from a more standardised approach to metabolic challenge and the prioritization of data generated using congenic littermate controls.

Neuromuscular.

Evidence is rapidly accumulating for the role of MLKL in mouse models of neurological disease. *Mlkl*$^{-/-}$ mice were reported to be protected in one model of chemically-induced Parkinson's disease, with a significantly attenuated neurotoxic inflammatory response contributing to higher dopamine levels (Q. S. Lin et al., 2020). Strikingly, recent evidence suggests that MLKL may be important for tissue regeneration following acute neuromuscular injury (Zhou et al., 2020) (Ying et al., 2018). In a model of cardiotoxin-induced muscle injury, muscle regeneration is driven by necroptotic muscle fibres releasing factors into the muscle stem cell microenvironment (Zhou et al., 2020). *Mlkl*$^{-/-}$ mice accumulate massive death-resistant myofibrils at the injury site (Zhou et al.,

2020). Furthermore, in a model of sciatic nerve injury, MLKL was reported as highly expressed by myelin sheath cells to promote break down and subsequent nerve regeneration (Ying et al., 2018). Overexpression of MLKL in this model is found to accelerate nerve regeneration (Ying et al., 2018), speaking to the potential of MLKL enhancing rather than blocking drugs in this area. However, contraindicating the use of MLKL activating drugs to mitigate neurological disease is the observation that MLKL accelerates demyelination in a necroptosis-independent fashion and thereby worsens multiple sclerosis pathology (S. Zhang et al., 2019). Finally, the role of necroptosis in murine amyotrophic lateral sclerosis remains contentious in the field. Wang et al., 2020 reported that MLKL-dependent necroptosis appears dispensable in the onset, progression and survival of $SOD1^{G93A}$ mice. Yet, there have been robust studies suggesting RIPK1-RIPK3-MLKL drives axonal pathology in both $SOD1^{G93A}$ and *Optn*$^{-/-}$ mice (Ito et al., 2016) (Chevin & Sébire, 2021). While opinions in the field still remain split on the relative contribution of MLKL in hematological vs non-hematological cells in many of these models, disorders of the neuromuscular system have clearly come to the fore in commercial necroptosis drug development efforts.

Haematological.

Mlkl$^{-/-}$ mice are haematologically indistinguishable from wild-type at steady state (Murphy et al., 2013) (Müller et al., 2017) (Tanzer et al., 2015). This trend continues as the mice age to 100 days (Alvarez-Diaz et al., 2016). Properly regulated necroptosis, however, is indispensable for haematological homeostasis. *Mlkl*$^{D139V/D139V}$ mice (which encode a constitutively active form of MLKL that functions independently of upstream activation from RIPK3) have severe deficits in platelet, lymphocyte and haematopoietic stem cell counts (Hildebrand et al., 2020). Mice expressing even one

Preprints (www.preprints.org) | NOT PEER-REVIEWED | Posted: 5 May 2021 doi:10.20944/preprints202105.0053.v1

copy of this *Mlkl*^{D139V} allele are unable to effectively reconstitute the haematopoietic system following sub-lethal irradiation or in competitive reconstitution studies (Hildebrand et al., 2020). Like *Ripk3*$^{-/-}$, mice, *Mlkl*$^{-/-}$ mice display a prolonged bleeding time and thus unstable thrombus formation (Y. Zhang et al., 2017) (Moujalled et al., 2021). MLKL, however, appears to play an additional, RIPK3-independent, role in platelet formation/clearance. In a model of lymphoproliferative disorder, *Casp8*$^{-/-}$*Mlkl*$^{-/-}$ double knockout mice develop a severe thrombocytopaenia that worsens with age (measured at 50 and 100 days) (Alvarez-Diaz et al., 2016). This phenotype is not observed in age-matched *Casp8*$^{-/-}$*Ripk3*$^{-/-}$ mice (Alvarez-Diaz et al., 2016). Finally, MLKL has also been shown to function in neutrophil NET-formation at the cellular level (D'Cruz et al., 2018) and *Mlkl*$^{-/-}$ mice are seen to be protected from diseases that implicate NET-formation; for example ANCA associated vasculitis (Schreiber et al., 2017) and deep vein thrombosis (Nakazawa et al., 2018).

Cancer and cancer treatment.

Cisplatin is a common chemotherapy that treats solid cancers although its utility is limited by its nephrotoxic effects (Y. Xu et al., 2015). Strikingly, *Mlkl*$^{-/-}$ mice are reported to be largely resistant to cisplatin-induced tubular necrosis compared to wild-type controls (Y. Xu et al., 2015). Athough mechanistically, it is still not understood how systemic delivery of a DNA-damaging agent such as cisplatin could induce renal necroptosis and whether it is particular to kidney tissue. Hematopoetic stem cells derived from *Mlkl*$^{-/-}$ mice play a key role in studies showing that apoptosis-resistant acute myeloid leukaemia (AML) could be forced to die via necroptosis (Brumatti et al., 2016). By adding a caspase inhibitor IDN-6556/emricasan, AML cells are sensitised to undergo necroptosis in response to known clinical inducer of apoptosis SMAC

mimetic, birinapant (Brumatti et al., 2016). IDN-6556/emricasan is well tolerated in humans (Hoglen et al., 2004), and is an excellent example of a therapeutic approach designed to enhance rather than block MLKL activity in vivo. Finally, the role of MLKL in intestinal tumorigenesis remains unclear; with studies proving MLKL is dispensable in both sporadic intestinal or colitis-associated cancer (Alvarez-Diaz et al., 2020) and yet, MLKL has been reported to have a protective effect in *Apc*$^{min/+}$ mice (Q. Zhao et al., 2019) by suppressing IL-6/JAK2/STAT3 signals (Q. Zhao et al., 2021).

Reproductive system.

There are two studies that assess the role of MLKL in age-induced male infertility. *Mlkl*$^{-/-}$ mice aged to 15 months demonstrate significantly reduced body, testicular and seminal vesicle weight alongside increased testosterone levels and fertility (Li et al., 2017) when compared to age matched wild-type mice. A recent follow up study suggests that CSNK1G2, a member of the casein kinase family, is co-expressed in the testes and inhibits necroptosis-mediated aging (Li et al., 2020). This phenomenon is also seen in human testes (Li et al., 2020). Another study that uses congenic littermate controls, however, finds that male mice aged to 18 months are indistinguishable from wild-type littermates with regards to total body, testicular and seminal vesicle weight (Webster et al., 2020).

Important experimental determinants in MLKL-related mouse research.

There are several high profile examples of genetic drift (Vanden Berghe, Kaiser, Bertrand, & Vandenabeele, 2015), passenger mutations (Vanden Berghe et al., 2015), facility-dependent variation in the microbiomes of mice (Robertson et al., 2019), sex (Klein & Flanagan, 2016) and age (Shaw, Goldstein, & Montgomery, 2013) acting as

Preprints (www.preprints.org) | NOT PEER-REVIEWED | Posted: 5 May 2021 doi:10.20944/preprints202105.0053.v1

important modifiers of the innate immune response. One notable example is the significant differences between commonly used wild-type control C567BL/6J and C57BL/6NJ (also known as C57BL/6N) sub-strains (separated by 60+ years of independent breeding) in morbidity and survival following LPS and TNF induced lethal shock (Vanden Berghe et al., 2015) (Newton et al., 2016). Of similar interest, a study finds male mice are more susceptible than females to invasive pneumonia and sepsis (Kadioglu et al., 2011). Generously powered cohorts of sex-segregated, co-housed, congenic littermates (mice derived from a heterozygous cross) are the gold standard for controlling all of these confounding variables when comparing wild-type and *Mlkl* KO/mutant mice (or any other mutant) (Robertson et al., 2019). All scientists that work with mice will attest that this approach is certainly time, resource and mouse-number intensive, it should nonetheless be prioritised by experimenters and peer reviewers alike wherever possible. We congratulate the efforts of scientists who proceed one step further by restoring the wild-type phenotype through ectopic expression of MLKL (Ying et al., 2018). When the use of littermate controls is not feasible, clear and detailed descriptions of mouse age, sex and provenance provided in publications act as important caveats for discerning reviewers and readers to consider. In Table 1, we summarize the outcomes of these comparisons in 80+ contexts and have included a column that provides details of caveats where available.

Concluding remarks.

Genetic and experimental models of disease provide a strong rationale that MLKL and necroptosis are important mediators and modifiers of infectious and non-infectious disease. The study of MLKL in mouse models has indicated a bidirectional role of necroptosis in disease. Inhibiting the function of MLKL may confer protection in

Preprints (www.preprints.org) | NOT PEER-REVIEWED | Posted: 5 May 2021 doi:10.20944/preprints202105.0053.v1

diseases characterised by haematopoietic dysfunction and uncontrolled inflammation borne of (and/or perpetuating) the failure of epithelial barriers throughout the body. Whereas enhancing MLKL-induced cell death may prove beneficial in the treatment of malignancies and nerve injury. The therapeutic potential of MLKL as a druggable target in infectious disease is highly nuanced and will require careful tailoring to the pathogen and infection site/stage in question. Importantly, any extrapolation of these observations in *Mlkl* knockout and mutant mice to human disease must be tempered by our knowledge of key differences in both the structure and regulation of mouse and human MLKL (Petrie et al., 2018) (Tanzer et al., 2016) (Davies et al., 2020). Rapid advances in the 'humanisation' of mouse models of disease and the use of large human clinico-genetic databases will further enrich the extensive body of murine data supporting the role of MLKL in human disease.

Preprints (www.preprints.org) | NOT PEER-REVIEWED | Posted: 5 May 2021 doi:10.20944/preprints202105.0053.v1

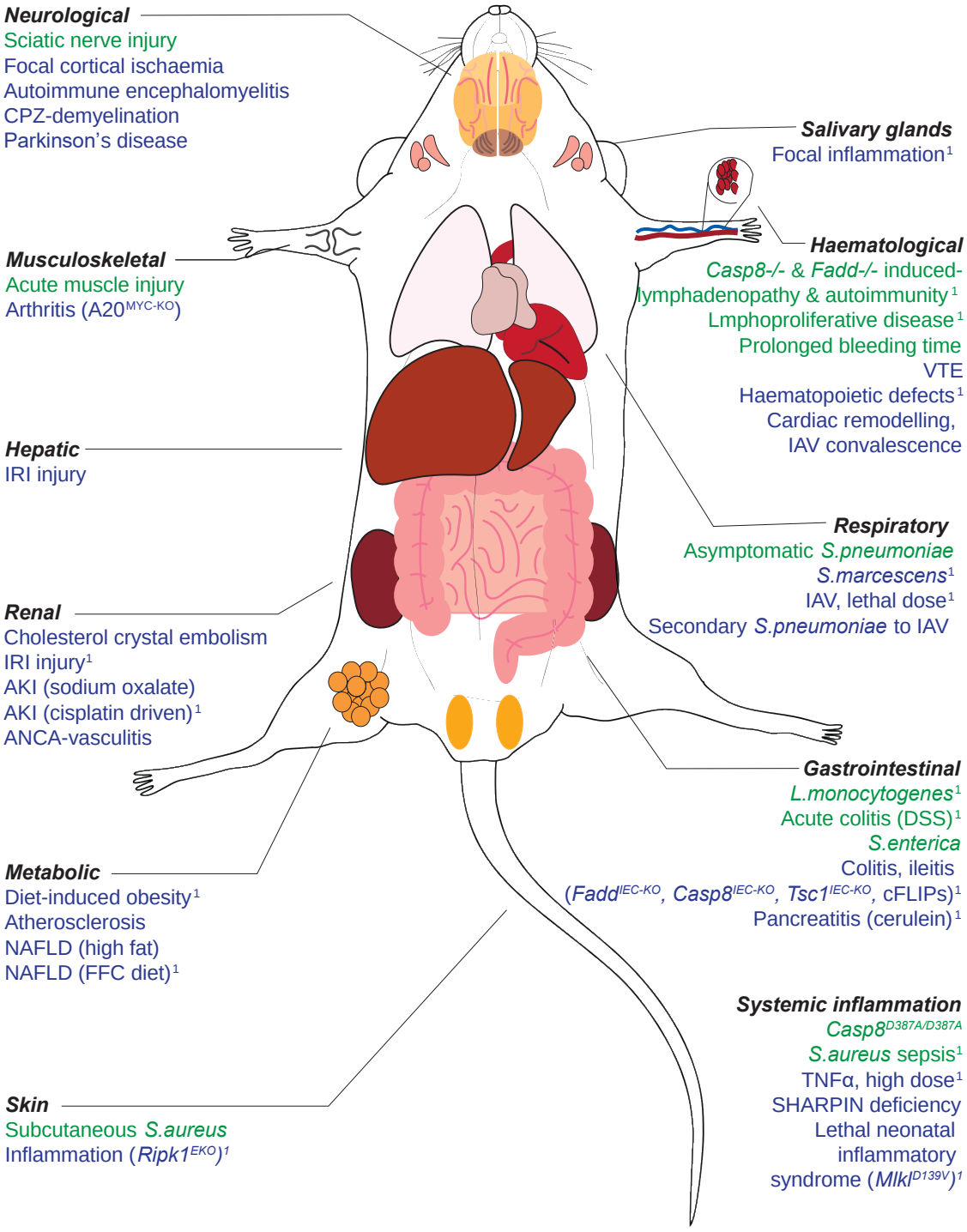

Figure 1: The role of necroptosis in infective and non-infective challenges spanning a wide array of physiological systems. Littermate controls utilised [1].

Preprints (www.preprints.org) | NOT PEER-REVIEWED | Posted: 5 May 2021 doi:10.20944/preprints202105.0053.v1

Table 1: Understanding the role of necroptosis in the aetiology of disease using *Mlkl*$^{-/-}$ and mutant mice.

Challenge	Method	Outcome in *Mlkl*$^{-/-}$ (mutant or knock-down) mouse relative to wild-type control	*Mlkl*$^{-/-}$ mice and wild-type control details	Reference
Ischemia and reperfusion injury (IRI)				
Hepatic IRI injury	45 min ischemia in chow- or western diet-fed mice.	Reduced TUNEL positive hepatocytes and serum ALT levels) in *Mlkl*$^{-/-}$ mice, irrespective of diet. Hepatic neutrophil infiltration TNF, IL-1, MIP-2 and IL-6 mRNA reduced post I/R in *Mlkl*$^{-/-}$ mice.	Sex-matched *Mlkl*$^{-/-}$ (CRISPR/Cas) and Wt mice utilised.	(Ni et al., 2019)
Renal infarction, no reperfusion	Cholesterol crystal embolism.	*Mlkl*$^{-/-}$ mice protected from infarction (measured by infarct size, kidney injury and neutrophil infiltration). No difference in the extent of acute kidney injury (measured by eGFR) and kidney failure.	*Mlkl*$^{-/-}$ (Murphy et al., 2013) and Wt mice utilised.	(Shi et al., 2020)
Renal IRI injury	40 min bilateral renal pedicle clamp.	*Mlkl*$^{-/-}$ mice protected from acute kidney injury (measured using serum creatinine and urea). *Ripk3*$^{-/-}$*/Mlkl*$^{-/-}$ double knockout mice were only somewhat protected.	Sex-, and weight-matched Wt controls for *Mlkl*$^{-/-}$ (Murphy et al., 2013) mice.	(Moerke et al., 2019)
	30 min renal pedicle clamp.	*Mlkl*$^{-/-}$ prolonged survival by ~4 days over Wt mice.	Male Wt and *Mlkl*$^{-/-}$ (Murphy et al., 2013) littermates.	(Newton et al., 2016)
Focal cortical ischaemia	Photothrombosis of the cortical microvessels.	Reduced infarction (fewer TUNEL/NeuN-positive cells) in *Mlkl*$^{-/-}$ mice and improved locomotion from day 7. Fewer F4/F8+ cells and reduced expression of iNOS, TNFα, IL-12 and IL-18.	*Mlkl*$^{-/-}$ sourced from Xiamen University*.	(Yang et al., 2018)
Sterile Inflammatory				
Acute kidney injury (AKI)	Intraperitoneal injection of sodium oxalate.	*Mlkl*$^{-/-}$ mice show reduced serum creatinine, neutrophil recruitment and tubular necrosis (TUNEL staining and tubular injury score).	Sex matched male Wt controls for *Mlkl*$^{-/-}$ (Murphy et al., 2013) mice.	(Mulay et al., 2016)

Preprints (www.preprints.org) | NOT PEER-REVIEWED | Posted: 5 May 2021 doi:10.20944/preprints202105.0053.v1

	Intraperitoneal injection of cisplatin.	*Mlkl*$^{-/-}$ mice resistant to tubular necrosis (histology, blood urea nitrogen and serum creatinine). Reduced TNFα, IL-1β, IFN-γ, IL-6 in proximal tubules despite similar levels to WT at baseline.	Male Wt and *Mlkl*$^{-/-}$ (TALEN) mice are littermates.	(Y. Xu et al., 2015)
Hepatitis	ConA-induced.	*Mlkl*$^{-/-}$ mice show reduced hepatocyte necrosis (TUNEL staining and ALT/AST). Driven by MLKL deficiency in hepatocytes (not immune cells).	Wt and *Mlkl*$^{-/-}$ (Murphy et al., 2013) a combination of C57BL/6J or littermate controls used.	(Günther et al., 2016)
		Hepatocyte necrosis in *Mlkl*$^{LPC\text{-}KO}$ mice, with specifically ablated MLKL in liver parenchymal cells, are indistinguishable from WT (ALT and H&E).	*Mlkl*$^{LPC\text{-}KO}$ and *Mlkl*$^{fl/fl}$ are littermates.	(Hamon et al., 2020)
	LPS/GalN-driven (model of apoptotic hepatitis).	*Mlkl*$^{-/-}$ mice are indistinguishable from WT (assessed using ALT/AST and histological staining for cleaved Casp3).	Wt and *Mlkl*$^{-/-}$ (Murphy et al., 2013) a combination of C57BL/6J or littermate controls used.	(Günther et al., 2016)
	Acetaminophen (model of drug-induced liver injury).	MLKL deficiency does not prevent liver injury (assessed using AST/ALT levels and TUNEL staining)	Wt and *Mlkl*$^{-/-}$ (Murphy et al., 2013) a combination of C57BL/6J or littermate controls used.	(Günther et al., 2016)
			Male Wt used for *Mlkl*$^{-/-}$ (Murphy et al., 2013) mice. Bred as separate cohorts.	(Dara et al., 2015)
Acute pancreatitis	Cerulein-induced.	*Mlkl*$^{-/-}$ mice experience less severe acinar cell necrosis than Wt mice (as measured by histological and quantitative analysis).	Male *Mlkl*$^{-/-}$ (TALEN) and Wt mice are littermates.	(J. Wu et al., 2013)
ANCA-driven necrotising crescent	αMPO IgG transfer.	*Mlkl*$^{-/-}$ mice were protected against NCGN (as measured by reduced leukocyturia, erythrocyturia and less crescents and necrotic change on histology)	*Mlkl*$^{-/-}$ (Murphy et al., 2013)*	(Schreiber et al., 2017)

Preprints (www.preprints.org) | NOT PEER-REVIEWED | Posted: 5 May 2021 doi:10.20944/preprints202105.0053.v1

glomerulo-nephritis				
Arthritis	K/B X N serum transfer.	No significant difference in disease progression between *Mlkl*$^{-/-}$ and WT mice (clinical severity scale and myeloperoxidase average radiance).	Sex matched Wt for *Mlkl*$^{-/-}$ mice.	(Lawlor et al., 2015)
	Myeloid-cell-specific A20 deficiency (A20^{MYC-KO}).	*Mlkl*$^{-/-}$, A20^{MYC-KO} mice were protected against inflammatory arthritis (thickness of rear ankles, histological scores of inflammation, cartilage and bone destruction), splenomegaly and showed reduced expression of IL-1B and TNFα.	Mice with loxP-flanked A20 crossed with Mlkl$^{-/-}$ (J. Lin et al., 2016) aged to 23-to-27 weeks old.	(Polykratis et al., 2019)
Colitis and ileitis	IEC-specific FADD and Caspase-8 deficiency.	*Mlkl*$^{-/-}$*Fadd*$^{IEC-KO}$ and *Mlkl*$^{-/-}$*Casp8*$^{IEC-KO}$ resistant to colitis. *Mlkl*$^{-/-}$*Casp8*$^{IEC-KO}$ are also resistant to ileitis whilst *Mlkl*$^{-/-}$*Fadd*$^{IEC-KO}$ are only partially protected. Assessed using histological analysis of colonic and ileal tissues and microarray).	Littermate control mice with homozygous or heterozygous loxP-flanked Fadd or Casp8.	(Schwarzer et al., 2020)
	IEC-specific highly active mTORC1 pathway (*Tsc1*$^{IEC-KO}$).	*Tsc1*$^{IEC-KO}$*Mlkl*$^{-/-}$ profoundly alleviates epithelial cell death and intestinal barrier dysfunction seen in *Tsc1*$^{IEC-KO}$.	*Tsc1*$^{IEC-KO}$ and *Tsc1*$^{IEC-KO}$*Mlkl*$^{-/-}$ were age- and sex-matched littermate controls.	(Xie et al., 2020)
Lethal ileitis	X-linked transgene -short form of cellular FLICE-inhibitory protein (cFLIPs).	MLKL deficiency partially rescues male mice from lethal in-utero ileitis (improved survival, small intestine villous architecture, fewer CC3-positive cells)	Male Wt and *Mlkl*$^{-/-}$ (Dannappel et al., 2014)	(Shindo et al., 2019)
Acute colitis	1.5% DSS in drinking water, 5 days, followed by 3 days of normal drinking water.	*Mlkl*$^{-/-}$ mice display increased weight loss, but only in some cohorts. Day 5 and 8, indistinguishable murine endoscopic index of colitis (MEIC) scores. Increased inflammation in the proximal colon and decreased submucosal inflammation in the distal colon (H&E).	Wt and *Mlkl*$^{-/-}$ (Murphy et al., 2013) are littermates.	(Alvarez-Diaz et al., 2020)

Preprints (www.preprints.org) | NOT PEER-REVIEWED | Posted: 5 May 2021 doi:10.20944/preprints202105.0053.v1

Inflammatory skin disease	RIPK1 deficient keratinocytes *Ripk1*^{EKO}.	Specific MLKL deficiency in keratinocytes profoundly ablated the development of the inflammatory skin lesion that invariably develops in *Ripk1*^{EKO} mice.	*Ripk1*$^{FL/FL}$ (Takahashi et al., 2014) *Mlkl*$^{FL/FL}$ (Murphy et al., 2013), wild-type littermates utilised.	(Devos et al., 2020)
Systemic inflammatory response syndrome (SIRS)	300µg/kg TNF intravenous/kg TND.	*Mlkl*$^{-/-}$ mice suffer a hypothermia reaction similar to that of WT controls.	WT and *Mlkl*$^{-/-}$ (Murphy et al., 2013) are littermates.	(Newton et al., 2016)
	500µg/kg TNF intravenous.	*Mlkl*$^{-/-}$ mouse core body temperature higher at 6, 8 and 10 hrs post dose than WT controls, indicating moderate protection.	WT and *Mlkl*$^{-/-}$ (Murphy et al., 2013) are littermates.	(Newton et al., 2016)
	30mg/kg LPS-intraperitoneal.	*Mlkl*$^{-/-}$ mice show similar serum TNF-a and IL-1β levels as WT (measured at 0, 2, 4 and 8 hours by ELISA).	Male *Mlkl*$^{-/-}$ (TALEN) and WT mice are littermates.	(J. Wu et al., 2013)
	1mg/kg TNFα in 200 µl PBS via the tail vein.	*Mlkl*$^{-/-}$ mice showed increased survival. *Ripk3*$^{-/-}$*Mlkl*$^{-/-}$ double knockout mice were not similarly protected.	Female WT and *Mlkl*$^{-/-}$ (Murphy et al., 2013) mice bred as separate cohorts.	(Moerke et al., 2019)
	50µg/kg LPS intraperitoneal.	*Mlkl*$^{-/-}$ mice showed comparable levels of TNFα and IL-6 (ELISA analysis) 1-hour post-treatment. Pre-treatment with necrostatin-1 (IV), 15 min prior to LPS, significantly reduced *Mlkl*$^{-/-}$ mice ability to produce TNFα and IL-6.	*	(Najjar et al., 2016)
Generalised inflammation	A20 gene deficiency.	*Mlkl*$^{-/-}$*A20*$^{-/-}$ mice display similar inflammation (hepatic neutrophil infiltration, RANTES secretion and dermatitis) and lifespan.	WT are *A20*$^{-/-}$ littermates.	(Newton et al., 2016)
TNF-induced multi-organ inflammation	SHARPIN deficiency *shpn*$^{m/m}$.	12-week-old *Shpn*$^{m/m}$*Mlkl*$^{-/-}$ mice show reduced liver inflammation and splenomegaly and leucocytosis in comparison to *Shp*$^{m/m}$ controls (histology, ADVIA automated haematological analysis).	C57BL/Ka *Shpn*$^{cpdm/cpdm}$ backcrossed to C57BL/6J one or two times or crossed with	(Rickard et al., 2014)

			C56BL/6J *Mlkl*$^{-/-}$ (Murphy et al., 2013) mice.	
Casp8$^{D387A/D387A}$ (non-cleavable caspase 8) induced **systemic inflammation**	*Casp8*$^{D387A/D387A}$ mutation.	*Mlkl*$^{-/-}$ *Casp8*$^{DA/DA}$ do not develop LPR disease. *Mlkl*$^{-/-}$ *Casp8*$^{DA/DA}$ show an exacerbated inflammatory phenotype with significant splenomegaly, liver damage (serum ALT, AST) and premature death.	*Casp8*$^{D387A/D387A}$ (CRISPR/Cas9) and *Mlkl*$^{-/-}$ (Murphy et al., 2013) mice. Sex-matched.	(Tummers et al., 2020)
Mlkl^{D139V} **induced lethal neonatal inflammatory syndrome**	Whole body homozygosity for constitutively active *Mlkl*^{D139V} mutation.	*Mlkl*^{D139V} homozygotes are born normal but develop acute multifocal inflammation of the head, neck and mediastinum by day P2/P3. Maximum lifespan observed 6 days.	Age and sex matched littermate controls.	(Hildebrand et al., 2020)
Infection				
Bacterial				
Staphylococcus aureus	Subcutaneous 2 x 10^6 CFU of *S.aureus* strain MRSA USA300.	5 days p.i. *Mlkl*$^{-/-}$ mice suffer greater bacterial burdens, larger skin lesions, significantly increased neutrophil, macrophage and $\gamma\delta$ T cell infiltrate and enhanced pro-inflammatory cytokine expression.	Sex-matched Wt and *Mlkl*$^{-/-}$ (Murphy et al., 2013).	(Kitur et al., 2016)
	Retro-orbital 1x 10^8 CFU *S.aureus* strain MRSA USA300.	*Mlkl*$^{-/-}$ mice show increased mortality rates compared to WT (a mean survival of 4 days).	Sex-matched Wt and *Mlkl*$^{-/-}$ (Murphy et al., 2013).	(Kitur et al., 2016)
	Intravenous 1x 10^7 CFU of *S.aureus* strain MRSA.	Accelerated weight loss and morbidity in *Mlkl*$^{-/-}$ mice. Circulating neutrophil numbers elevated 24 hours p.i.. Increased CFU in the blood of KO mice and MRSA burden in the kidney.	*Mlkl*$^{-/-}$ (Murphy et al., 2013) mice littermates utilised.	(D'Cruz et al., 2018)
	Retro-orbital 1x 10^{6-7} CFU of *S.aureus* strain MRSA.	*Mlkl*$^{-/-}$ mice show increased MRSA burden in blood and kidneys and greater number of peripheral neutrophils (flow cytometry).	*Mlkl*$^{-/-}$ (Murphy et al., 2013) mice littermates utilised.	(D'Cruz et al., 2018)

Preprints (www.preprints.org) | NOT PEER-REVIEWED | Posted: 5 May 2021 doi:10.20944/preprints202105.0053.v1

	Intraperitoneal 1 x 10^7 CFU of *S.aureus* strain MRSA.	*Mlkl*$^{-/-}$ mice display more severe bacteraemia 24 hours p.i.	*Mlkl*$^{-/-}$ (Murphy et al., 2013) mice littermates utilised.	(D'Cruz et al., 2018)
Mycobacterium tuberculosis	~100-200 CFU of *Mtb* via aerosol strain H37Rv.	*Mlkl*$^{-/-}$ mice are indistinguishable from WT controls in terms of splenic & respiratory bacterial burden, gross lung histopathology of inflammatory lesions (number & size), organisation of granulomatous inflammation, immune cell counts, TNFα and IL-1β.	Sex-matched Wt and *Mlkl*$^{-/-}$ (Murphy et al., 2013) mice.	(Stutz et al., 2018)
Polymicrobial septic shock	Cecal ligation and puncture (CLP).	*Mlkl*$^{-/-}$ and WT mice showed same survival profile (mortality was monitored from 24 hours to 144 hours).	Age- and sex-matched littermates of Wt and *Mlkl*$^{-/-}$.	(J. Wu et al., 2013)
Acute kidney injury (AKI) following polymicrobial septic shock	Cecal ligation and puncture (CLP).	*Mlkl*$^{-/-}$ mice suffer same extent of AKI. Ratio of lipocalin-2/urine creatinine levels were lower in *Mlkl*$^{-/-}$ mice than WT, however not as reduced as *Ripk3*$^{-/-}$ mice.	Wt and *Mlkl*$^{-/-}$ (Jiahuai Han laboratory) littermates.	(Sureshbabu et al., 2018)
Asymptomatic chronic nasopharyngeal colonisation with *S. pneumoniae*	Nasal instillation of ~1 x 10^5 CFU of serotype 4 strain TIGR4 μ.	*Mlkl*$^{-/-}$ mice demonstrated reduced nasopharyngeal epithelial cell sloughing and increased LDH, Il-33, IL-1α, CXCL2 levels and decreased Il-6, Il-17 and polymorphonuclear cells than WT. *lkl*$^{-/-}$ mice cleared *S. pneumoniae* colonisation at a slower rate than WT controls. Less anti-PspA IgG than WT controls despite comparable total serum IgG concentration.	Wt and *Mlkl*$^{-/-}$ (Murphy et al., 2013) mice utilised.	(Riegler et al., 2019)
***S. marcescens* haemorrhagic pneumonia**	Intratracheal infection with strain MB383.	*Mlkl*$^{-/-}$ mice have increased alveolar macrophages and suffer less lung damage (histological analysis).	Wt and *Mlkl*$^{-/-}$ littermates (Douglas Green).	(González-Juarbe et al., 2015)
Listeria Monocytogenes	Oral 1 x 10^8 CFU *L.monocytogenes*	3 days p.i. *Mlkl*$^{-/-}$ mice have a moderate increase in liver bacterial colonisation compared to WT littermate controls.	Female Wt and *Mlkl*$^{-/-}$ (Murphy et al., 2013) littermates.	(Sai et al., 2019)

Preprints (www.preprints.org) | NOT PEER-REVIEWED | Posted: 5 May 2021 doi:10.20944/preprints202105.0053.v1

	1/2b strain 2011L-2858.			
Salmonella enterica	Oral $5x10^7$ CFU - $1x10^8$ CFU *Subsp. Enterica serovar Typhimurium* strain SL1344.	*Mlkl*$^{-/-}$ mice show increased greater submucosal oedema, loss of goblet cells, PMN infiltration, loss of epithelial barrier integrity and greater salmonella colonisation despite comparable bacterial faecal loads. Also have increased body and caecal weight loss.	Wt and *Mlkl*$^{-/-}$ (Dr. Jia-Huai Han, Xiamen University, China) were sex-matched.	(Yu et al., 2018)
Viral				
Influenza A strain PR8	Instranasal 4,000 EID50.	*Mlkl*$^{-/-}$ mice indistinguishable from WT in terms of survival (75% of both *Mlkl*$^{-/-}$ and WT mice survived and recovered) and lung progeny virion output.	Sex-matched WT controls*.	(Nogusa et al., 2016)
	Instranasal 2,500 EID_{50}. Intranasal 6000 EID_{50}.	*Mlkl*$^{-/-}$ mice are indistinguishable from WT in terms of survival. At this lethal dose, *Mlkl*$^{-/-}$ mice show increased survival; fewer disrupted epithelial cells despite same viral titre 6 days p.i. Influx of neutrophils into the lungs in *Mlkl*$^{-/-}$ mice both delayed and diminished.	Sex-matched littermates used for *Mlkl*$^{-/-}$ mice (Murphy et al., 2013).	(T. Zhang et al., 2020)
	Instranasal 2,500 EID_{50}. Instranasal 1,500 EID_{50}.	*Mlkl*$^{-/-}$ are indistinguishable from WT controls in terms of survival, viral titres, morphometry of viral spread and percentage of infected lung. IAV-mediated alveolar inflammation; septal thickening, inflamed alveoli and hyaline membranes in *Mlkl*$^{-/-}$ mice comparable to that of WT mice.	Sex matched Wt littermate or Wt C57BL/6 mice were used as controls for *Mlkl*$^{-/-}$ mice (Murphy et al., 2013).	(Shubina et al., 2020)
Influenza strain A/California/7/2009	250 PFU of IAV.	At baseline, *Mlkl*$^{-/-}$ mouse myocardium showed increased mitochondrial and antioxidant activity (proteome analysis), increased survival and reduced weight loss.	Wt (B6NTac) mice and *Mlkl*$^{-/-}$ mice (Murphy et al., 2013) were bred independently.	(Y. H. Lin et al., 2021)

Preprints (www.preprints.org) | NOT PEER-REVIEWED | Posted: 5 May 2021 doi:10.20944/preprints202105.0053.v1

Secondary *S. pneumoniae* following Influenza A viral infection	Intranasal 250 PFU pdmH1N1. Intratracheal 1x 10^3 CFU of *S. pneumoniae*.	*Mlkl*$^{-/-}$ mice showed reduced-pulmonary cell death (TUNEL-staining), -bacterial burden, -lung consolidation, -IFN-α and -B expressed. No changes in the amount of oxidative-stress-induced DNA damage (immunofluorescence of 8-OHdG).	Wt and *Mlkl*$^{-/-}$ (Murphy et al., 2013).	(Gonzalez-Juarbe et al., 2020)
West Nile Virus (WNV) encephalitis	Subcutaneous injection with 100 pfu of WNV-TX 2002-HC strain.	*Mlkl*$^{-/-}$ mice are indistinguishable from WT in terms of survival and viral titres.	Sex matched Wt C57BL/6J used for *Mlkl*$^{-/-}$ mice (Murphy et al., 2013).	(Daniels et al., 2017)
Metabolic				
Non-alcoholic fatty liver disease	Choline-deficient, methionine-supplemented (CDE), fed once.	*Mlkl*$^{-/-}$ mice were indistinguishable from WT controls in terms of hepatic necrosis (serum AST and PI-positive cells). Reduced systemic levels of Il-6 and IL-1β (RT-PCR), comparable levels of TNFα.	Male C57BL/6J (CLEA Japan) including *Mlkl*$^{-/-}$ *(*M.Pasparakis) were utilised.	(Tsurusaki et al., 2019)
	12 weeks of high fat diet.	*Mlkl*$^{-/-}$ mice gain body weight comparable to WT. At baseline, *Mlkl*$^{-/-}$ mice had increased serum AST/ALT and decreased serum fasting blood glucose. *Mlkl*$^{-/-}$ mice demonstrate reduced; NAFLD activity score, steatosis score, hepatocyte ballooning, lobular inflammation, serum AST/ALT, triglyceride levels, de novo fat synthesis.	C57BL/6N Wt and *Mlkl*$^{-/-}$ (Jiahuai Han) mice utilised.	(Saeed et al., 2019)
	8 weeks of western diet.	*Mlkl*$^{-/-}$ are indistinguishable from WT in terms of level of steatosis and liver triglyceride accumulation.	Sex-matched *Mlkl*$^{-/-}$ (CRISPR/Cas) on C57BL/6N and Wt utilised.	(Ni et al., 2019)
	12 weeks of fat, fructose and cholesterol (FFC) diet.	*Mlkl*$^{-/-}$ mice are protected from liver injury (measured using AST/ALT, hepatic triglyceride accumulation, macrovesicular & microvesicular steatosis (H&E). *Mlkl*$^{-/-}$ mice were protected from FFC-induced apoptosis (measured using M30 levels, cleaved caspase-3 and TUNEL-positive cells) and	Littermates utilised.	(X. Wu et al., 2020)

Preprints (www.preprints.org) | NOT PEER-REVIEWED | Posted: 5 May 2021 doi:10.20944/preprints202105.0053.v1

		inflammation (measured using mRNA levels of *Tnfa, Il-1β Mcp-1* and *F4/80*).		
Alcoholic fatty liver disease (ALFD)	Chronic ethanol-induced.	*Mlkl*$^{-/-}$ mice are indistinguishable from WT in terms of ALT/AST, hepatic triglycerides, macrovesicular & microvesicular steatosis (H&E).	Sex-matched littermates utilised.	(Miyata et al., 2021)
	Gao-binge.	*Mlkl*$^{-/-}$ mice are indistinguishable from WT in terms of body weights, food intake, ALT/AST, hepatic triglycerides, macrovesicular & microvesicular steatosis (H&E). *Mlkl*$^{-/-}$ mice have similar levels of CYP2E1, ER stress and hepatocyte apoptosis but mildly reduced levels of some hepatic inflammatory markers.	Sex-matched littermates utilised.	(Miyata et al., 2021)
Diet-induced obesity	16 weeks of high fat diet (HFD) consisting of 60% kcal from fat or chow diet (CD).	*Mlkl*$^{-/-}$ mice on regular CD are indistinguishable from WT littermates in terms of body weight, glucose disposal, glucose tolerance, or insulin sensitivity After 16 weeks on HFD, *Mlkl*$^{-/-}$ mice have lower body weight, and visceral adipose, better glucose and insulin tolerance. No difference in inflammatory markers or TUNEL positive cells in the liver.	Body weight matched, male Wt and *Mlkl*$^{-/-}$ littermates are utilised.	(H. Xu et al., 2019)
Atherosclerosis	Western diet for 8 or 16 weeks.	*Apoe*$^{-/-}$ mice fed a western diet while receiving MLKL antisense oligonucleotides (ASOs) demonstrated reduced necrotic cores size of aortic sinus plaques, reduced plasma cholesterol, fewer TUNEL positive cells but increased lipid content in atherosclerotic plaque (oil red O staining).	*Apoe*$^{-/-}$ C57Bl/6N mice administered with control or MLKL antisense oligonucleotides (ASOs).	(Rasheed et al., 2020)
Neoplasia				
Acute myeloid leukaemia	Retroviral expression of the fusion protein (MLL-ENL) in *Mlkl*$^{-/-}$	AML cells (MLL-ENL-transduced E14 liver hematopoietic stem cells (HSCs) transplanted into lethally irradiated WT mice. AML generated from *Mlkl*$^{-/-}$ HSCs showed similar leukemia progression and overall survival compared to AML generated from WT HSCs.	Age matched, both *Mlkl*$^{-/-}$ and Wt on C57B/6J background.	(Brumatti et al., 2016)

Preprints (www.preprints.org) | NOT PEER-REVIEWED | Posted: 5 May 2021 doi:10.20944/preprints202105.0053.v1

	haematopoietic stem cells.			
Colon cancer	Sporadic intestinal adenoma (APC^{min} mouse).	No significant difference in colonic tumour burden or tumour number. No difference in colonic inflammation (H&E) or expression of Il-6.	Wt and *Mlkl*$^{-/-}$ (Murphy et al., 2013) are littermates. Data for both sexes presented.	(Alvarez-Diaz et al., 2020)
	Colitis-associated cancer (azoxymethane, DSS).	No significant difference in weight loss observed. Similar timing of tumour onset and burden between *Mlkl*$^{-/-}$ and Wt (endoscopic tumour scores and H&E).	Wt and *Mlkl*$^{-/-}$ (Murphy et al., 2013) are littermates. Data for both sexes presented.	(Alvarez-Diaz et al., 2020)
Colitis-associated tumorigeneses	AOM injection at 10mg/kg of body weight. 5 days post, fed with three cycle of 3% (w/v) DSS, followed by 14 days of normal water.	*Mlkl*$^{-/-}$ mice have a significant reduction in body weight, increased clinical severity, shorter colons and worse survival in comparison to Wt. *Mlkl*$^{-/-}$ mice exhibit increased burden of anal and colonic polyps with significant increase in inflammation, hyperplasia and dysplasia (H&E).	Wt and *Mlkl*$^{-/-}$ (CRISPR-Cas9) were sex-matched (males only).	(Q. Zhao et al., 2019)
		Apc$^{min/+}$*Mlkl*$^{-/-}$ mice have a median survival time on 127 days compared with *Apc*$^{min/+}$survival of 185 days, alongside marked increased in tumour number and load.	Wt and *Mlkl*$^{-/-}$ (CRISPR-Cas9) were littermate controls.	(Q. Zhao et al., 2021)
Progressive lymphoproliferative disease	*Fadd* gene knock out.	*Mlkl* gene knockout rescues *Fadd*$^{-/-}$ mice from embryonic lethality, but results in more severe progressive lymphoproliferative disease compared to *Ripk3*$^{-/-}$ *Fadd*$^{-/-}$ mice.	*Mlkl*$^{-/-}$ *generated by* CRISPR-Cas9 (Bioray Labs).	(X. Zhang et al., 2016)
			Littermates derived from *Fadd*$^{+/-}$, *Mlkl*$^{+/-}$ crosses (Murphy et al., 2013) mice utilised.	(Alvarez-Diaz et al., 2016)

Preprints (www.preprints.org) | NOT PEER-REVIEWED | Posted: 5 May 2021 doi:10.20944/preprints202105.0053.v1

	Casp8 gene knock out.	*Mlkl* gene knockout rescues *Casp8*$^{-/-}$ mice from embryonic lethality, but results in more severe progressive lymphoproliferative disease compared to *Ripk3*$^{-/-}$ *Casp8*$^{-/-}$ mice.	Littermates derived from *Casp8*$^{+/-}$, *Mlkl*$^{+/-}$ crosses (Murphy et al., 2013) mice utilised.	(Alvarez-Diaz et al., 2016)
Neuromuscular				
Amyotrophic lateral sclerosis	*SOD1*^{G93A} mice (express mutant human superoxide dismutase 1).	MLKL deficiency does not affect disease onset, progression or survival in *SOD1*^{G93A} mice. MLKL ablation has no impact on astrocyte or microglial activation.	Four isogenic genotypes for study: *SOD1*^{G93A}*; Mlkl*$^{-/-}$, *SOD1*^{G93A}*, Mlkl*$^{-/-}$, and WT littermates. *Mlkl*$^{-/-}$ mice (Murphy et al., 2013).	(Wang et al., 2020)
Sciatic nerve crush injury	Sciatic nerve cut or crushed unilaterally.	pMLKL (serine 441) is upregulated in damaged sciatic nerve cells of both WT and *Ripk3*$^{-/-}$ mouse sciatic nerves. *Mlkl*$^{-/-}$ mice suffer drastically reduced myelin sheath breakdown and thus reduced sciatic nerve regeneration and function.	Male only *Mlkl*$^{-/-}$ (Li et al., 2017) and Wt (C57BL/6J) utilised.	(Ying et al., 2018)
Experimental autoimmune encephalomyelitis EAE	Intraperitoneal injection of 200 ng of pertussis toxin.	*Mlkl*$^{-/-}$ mice display significantly reduced clinical EAE disease scores with delayed reduction of myelination (MBP immunofluorescence).	Sex matched Wt and *Mlkl*$^{-/-}$ (CRISPR Cas9) bred as separate cohorts. Same housing conditions since birth.	(S. Zhang et al., 2019)
Cuprizone CPZ – induced demyelination	Fed 0.2% CPZ in chow for 4 weeks.	*Mlkl*$^{-/-}$ mice have delayed demyelination in the caudal corpus callosum (MBP immunofluorescence).	Sex matched Wt and *Mlkl*$^{-/-}$ (CRISPR Cas9) bred as separate cohorts. Same housing conditions since birth.	(S. Zhang et al., 2019)

Preprints (www.preprints.org) | NOT PEER-REVIEWED | Posted: 5 May 2021 doi:10.20944/preprints202105.0053.v1

Parkinson's disease (PD)	Intraperitoneal injection of MPTP.	*Mlkl*$^{-/-}$ show reduced neuroinflammatory markers (TNF-, IL-1β and IL-1 mRNA) and are significantly protected from striatal dopamine reduction and TH-positive neuron loss from the substantia nigra pars compacta compared to WT controls.	Male *Mlkl*$^{-/-}$ (Jiahuai Han, Xiamen Univeristy, China) and Wt utilised.	(Q. S. Lin et al., 2020)
Acute muscle injury	Intramuscular injection of cardiotoxin (CTX).	*Mlkl*$^{-/-}$ mice have fewer active muscle stem cells significantly impaired capacity to regenerate muscle fibres. Regenerating myofibrils from *Mlkl*$^{-/-}$ mice expressed significantly less myogenic factors MyoD, MyoG and nascent myofibril marker MYH3 in contrast to WT.	Male *Mlkl*$^{-/-}$ (CRISPR/Cas9) and Wt mice utilised.	(Zhou et al., 2020)
Haematological				
Venous thromboembolic (VTE) disease	100% flow obstruction of the IVC using ETHICON.	*Mlkl*$^{-/-}$ mice develop significantly smaller thrombi, with reduced areas of TUNEL+ cells, Ly6b+ neutrophils and F4/80+ macrophages. Systemically, *Mlkl*$^{-/-}$ mice have fewer circulating neutrophils, monocytes and serum histone-DNA complexes following IVC ligation. No difference in baseline number of neutrophils, monocytes, DAMPs or bleeding time.	Male Wt (C57BL/6N) and *Mlkl*$^{-/-}$ (Murphy et al., 2013).	(Nakazawa et al., 2018)
Baseline	*Mlkl*$^{-/-}$ mice aged to 50 and 100 days.	MLKL KO mice are indistinguishable from WT, for the blood parameters: WBC & lymphocyte count, thymic weight and cell count, splenic weight and cell count, lymph node weight and cell count.	Littermates derived from *Casp8*$^{+/-}$, *Mlkl*$^{+/-}$ crosses (Murphy et al., 2013) mice utilised.	(Alvarez-Diaz et al., 2016)
Casp8 or FADD deficiency	Casp8 or FADD deficient background.	Compared with *Casp8*$^{-/-}$*Ripk3*$^{-/-}$ or *Fadd*$^{-/-}$*Ripk3*$^{-/-}$ mice, the *Casp8*$^{-/-}$*Mlkl*$^{-/-}$ or *Fadd*$^{-/-}$*Mlkl*$^{-/-}$ demonstrate more severe lymphadenopathy and autoimmune manifestations.	Littermates derived from *Casp8*$^{+/-}$, *Mlkl*$^{+/-}$ crosses (Murphy et al., 2013) mice utilised.	(Alvarez-Diaz et al., 2016)
Reconstitution of the haematopoietic system	Competitive transplantation assay using	Following myeloablation, *Mlkl*$^{-/-}$ bone marrow stem cells were able to compete effectively with wild-type counterparts for reconstitution of the haematopoietic system (blood, bone marrow and spleen).	Littermate controls.	(Murphy et al., 2013)

Preprints (www.preprints.org) | NOT PEER-REVIEWED | Posted: 5 May 2021 doi:10.20944/preprints202105.0053.v1

	myeloablated recipients.			
***Mlkl*^{D139V} induced hematopoietic defects**	Whole body homozygosity for constitutively active *Mlkl*^{D139V} mutation.	P3 *Mlkl*$^{D139V/D139V}$ mice had significant deficits in lymphocyte and platelet counts in comparison to P3 *Mlkl*$^{Wt/Wt}$ and *Mlkl*$^{D139V/Wt}$.	Age and sex matched littermate controls.	(Hildebrand et al., 2020)
	Myelosuppressive irradiation.	Recovery was delayed in *Mlkl*$^{Wt/D139V}$ adult mice.	Age and sex matched littermate controls.	(Hildebrand et al., 2020)
	5-fluorouracil.	Adult *Mlkl*$^{D139V/Wt}$ mice had delayed recovery of haematopoietic stem and progenitor cells.	Age and sex matched littermate controls.	(Hildebrand et al., 2020)
	Competitive bone marrow transplants.	Bone marrow- derived HSCs from *Mlkl*$^{Wt/D139V}$ adults and fetal liver- derived HSCs from *Mlkl*$^{Wt/D139V}$ and *Mlkl*$^{D139V/D139V}$competed poorly or not at all with co-transplanted WT bone marrow.	Age and sex matched littermate controls.	(Hildebrand et al., 2020)
Acute thrombocytopaenia	Single dose of anti-platelet serum.	*Mlkl*$^{-/-}$ recovery of similarly to wild-type, in terms of magnitude and kinetics magnitude and kinetics to wild type mice.	Wt and *Mlkl*$^{-/-}$ (Murphy et al., 2013)	(Moujalled et al., 2021)
Haemostasis	Bleed times into 37°C saline, after 3-mm tail amputations, measured over 10 min	*Mlkl*$^{-/-}$ show prolonged bleeding time compared to wild-type and yet, equivalent total blood loss.	Wt and *Mlkl*$^{-/-}$ (Murphy et al., 2013)	(Moujalled et al., 2021)
Reproductive system				
Male reproductive system aging	Male mice aged 15 months.	*Mlkl*$^{-/-}$ mice showed reduced body weight, reduced seminal vesicle weight, increased testosterone, increased fertility, fewer empty seminiferous tubules.	Wt and *Mlkl*$^{-/-}$ (CRISPR Cas9) bred as separate cohorts. Same housing conditions since birth.	(Li et al., 2017)

Preprints (www.preprints.org) | NOT PEER-REVIEWED | Posted: 5 May 2021 doi:10.20944/preprints202105.0053.v1

	Male mice aged 18 months.	No significant difference in mortality, body weight, testis weight, seminal vesicle weight or germ cell loss in seminiferous tubules between *Mlkl*$^{-/-}$ mice and WT mice.	Wt and *Mlkl*$^{-/-}$ (Murphy et al., 2013) mice derived from heterozygous inter-cross (litter-mate controls).	(Webster et al., 2020)
Other				
Ventilator-induced lung injury (VILI)		*Mlkl*$^{-/-}$ mice were not protected against VILI at low or high tidal volumes.	Littermate Wt used for *Mlkl*$^{-/-}$ (Jiahuai Han Laboratory) mice.	(Siempos et al., 2018)
Progressive renal fibrosis	Left urethral obstruction (UUO) by double ligation.	*Mlkl*$^{-/-}$ mice were not protected from renal damage.	Sex-matched male Wt and *Mlkl*$^{-/-}$ (Jiahuai Han Laboratory) mice.	(Imamura et al., 2018)

*Methods not available

References:

Alvarez-Diaz, S., Dillon, C. P., Lalaoui, N., Tanzer, M. C., Rodriguez, D. A., Lin, A., . . . Strasser, A. (2016). The Pseudokinase MLKL and the Kinase RIPK3 Have Distinct Roles in Autoimmune Disease Caused by Loss of Death-Receptor-Induced Apoptosis. *Immunity, 45*(3), 513-526. doi:10.1016/j.immuni.2016.07.016

Alvarez-Diaz, S., Preaudet, A., Samson, A. L., Nguyen, P. M., Fung, K. Y., Garnham, A. L., . . . Murphy, J. M. (2020). Necroptosis is dispensable for the development of inflammation-associated or sporadic colon cancer in mice. *Cell Death Differ*. doi:10.1038/s41418-020-00673-z

Brumatti, G., Ma, C., Lalaoui, N., Nguyen, N. Y., Navarro, M., Tanzer, M. C., . . . Silke, J. (2016). The caspase-8 inhibitor emricasan combines with the SMAC mimetic birinapant to induce necroptosis and treat acute myeloid leukemia. *Sci Transl Med, 8*(339), 339ra369. doi:10.1126/scitranslmed.aad3099

Chevin, M., & Sébire, G. (2021). Necroptosis in ALS: a hot topic in-progress. *Cell Death Discovery, 7*(1), 79. doi:10.1038/s41420-021-00458-4

D'Cruz, A. A., Speir, M., Bliss-Moreau, M., Dietrich, S., Wang, S., Chen, A. A., . . . Croker, B. A. (2018). The pseudokinase MLKL activates PAD4-dependent NET formation in necroptotic neutrophils. *Sci Signal, 11*(546). doi:10.1126/scisignal.aao1716

Daniels, B. P., Snyder, A. G., Olsen, T. M., Orozco, S., Oguin, T. H., 3rd, Tait, S. W. G., . . . Oberst, A. (2017). RIPK3 Restricts Viral Pathogenesis via Cell Death-Independent Neuroinflammation. *Cell, 169*(2), 301-313.e311. doi:10.1016/j.cell.2017.03.011

Dannappel, M., Vlantis, K., Kumari, S., Polykratis, A., Kim, C., Wachsmuth, L., . . . Pasparakis, M. (2014). RIPK1 maintains epithelial homeostasis by inhibiting apoptosis and necroptosis. *Nature, 513*(7516), 90-94. doi:10.1038/nature13608

Dara, L., Johnson, H., Suda, J., Win, S., Gaarde, W., Han, D., & Kaplowitz, N. (2015). Receptor interacting protein kinase 1 mediates murine acetaminophen toxicity independent of the necrosome and not through necroptosis. *Hepatology, 62*(6), 1847-1857. doi:10.1002/hep.27939

Davies, K. A., Fitzgibbon, C., Young, S. N., Garnish, S. E., Yeung, W., Coursier, D., . . . Murphy, J. M. (2020). Distinct pseudokinase domain conformations underlie divergent activation mechanisms among vertebrate MLKL orthologues. *Nat Commun, 11*(1), 3060. doi:10.1038/s41467-020-16823-3

Devos, M., Tanghe, G., Gilbert, B., Dierick, E., Verheirstraeten, M., Nemegeer, J., . . . Maelfait, J. (2020). Sensing of endogenous nucleic acids by ZBP1 induces keratinocyte necroptosis and skin inflammation. *J Exp Med, 217*(7). doi:10.1084/jem.20191913

Doerflinger, M., Deng, Y., Whitney, P., Salvamoser, R., Engel, S., Kueh, A. J., . . . Herold, M. J. (2020). Flexible Usage and Interconnectivity of Diverse Cell Death Pathways Protect against Intracellular Infection. *Immunity, 53*(3), 533-547.e537. doi:10.1016/j.immuni.2020.07.004

Dondelinger, Y., Hulpiau, P., Saeys, Y., Bertrand, M. J. M., & Vandenabeele, P. (2016). An evolutionary perspective on the necroptotic pathway. *Trends Cell Biol, 26*(10), 721-732. doi:10.1016/j.tcb.2016.06.004

González-Juarbe, N., Gilley, R. P., Hinojosa, C. A., Bradley, K. M., Kamei, A., Gao, G., . . . Orihuela, C. J. (2015). Pore-Forming Toxins Induce Macrophage Necroptosis during Acute Bacterial Pneumonia. *PLoS Pathog, 11*(12), e1005337. doi:10.1371/journal.ppat.1005337

Gonzalez-Juarbe, N., Riegler, A. N., Jureka, A. S., Gilley, R. P., Brand, J. D., Trombley, J. E., . . . Orihuela, C. J. (2020). Influenza-Induced Oxidative Stress Sensitizes Lung Cells to Bacterial-Toxin-Mediated Necroptosis. *Cell Rep, 32*(8), 108062. doi:10.1016/j.celrep.2020.108062

GSK. (2019). *Q3 2019 Results* Retrieved from https://www.gsk.com/media/5745/q3-2019-results-slides.pdf

Günther, C., He, G. W., Kremer, A. E., Murphy, J. M., Petrie, E. J., Amann, K., . . . Wirtz, S. (2016). The pseudokinase MLKL mediates programmed hepatocellular necrosis independently of RIPK3 during hepatitis. *J Clin Invest, 126*(11), 4346-4360. doi:10.1172/jci87545

Hamon, A., Piquet-Pellorce, C., Dimanche-Boitrel, M. T., Samson, M., & Le Seyec, J. (2020). Intrahepatocytic necroptosis is dispensable for hepatocyte death in murine immune-mediated hepatitis. *J Hepatol, 73*(3), 699-701. doi:10.1016/j.jhep.2020.05.016

Hasegawa, T., Ito, Y., Wijeweera, J., Liu, J., Malle, E., Farhood, A., . . . Jaeschke, H. (2007). Reduced inflammatory response and increased microcirculatory disturbances during hepatic ischemia-reperfusion injury in steatotic livers of ob/ob mice. *Am J Physiol Gastrointest Liver Physiol, 292*(5), G1385-1395. doi:10.1152/ajpgi.00246.2006

Hildebrand, J. M., Kauppi, M., Majewski, I. J., Liu, Z., Cox, A. J., Miyake, S., . . . Silke, J. (2020). A missense mutation in the MLKL brace region promotes lethal neonatal inflammation and hematopoietic dysfunction. *Nat Commun, 11*(1), 3150. doi:10.1038/s41467-020-16819-z

Hoglen, N. C., Chen, L. S., Fisher, C. D., Hirakawa, B. P., Groessl, T., & Contreras, P. C. (2004). Characterization of IDN-6556 (3-[2-(2-tert-butyl-phenylaminooxalyl)-amino]-propionylamino]-4-oxo-5-(2,3,5,6-tetrafluoro-phenoxy)-pentanoic acid): a liver-targeted caspase inhibitor. *J Pharmacol Exp Ther, 309*(2), 634-640. doi:10.1124/jpet.103.062034

Imamura, M., Moon, J. S., Chung, K. P., Nakahira, K., Muthukumar, T., Shingarev, R., . . . Choi, M. E. (2018). RIPK3 promotes kidney fibrosis via AKT-dependent ATP citrate lyase. *JCI Insight, 3*(3). doi:10.1172/jci.insight.94979

Ito, Y., Ofengeim, D., Najafov, A., Das, S., Saberi, S., Li, Y., . . . Yuan, J. (2016). RIPK1 mediates axonal degeneration by promoting inflammation and necroptosis in ALS. *Science, 353*(6299), 603-608. doi:10.1126/science.aaf6803

Kadioglu, A., Cuppone, A. M., Trappetti, C., List, T., Spreafico, A., Pozzi, G., . . . Oggioni, M. R. (2011). Sex-based differences in susceptibility to respiratory and systemic pneumococcal disease in mice. *J Infect Dis, 204*(12), 1971-1979. doi:10.1093/infdis/jir657

Khandpur, R., Carmona-Rivera, C., Vivekanandan-Giri, A., Gizinski, A., Yalavarthi, S., Knight, J. S., . . . Kaplan, M. J. (2013). NETs are a source of citrullinated autoantigens and stimulate inflammatory responses in rheumatoid arthritis. *Sci Transl Med, 5*(178), 178ra140. doi:10.1126/scitranslmed.3005580

Kitur, K., Wachtel, S., Brown, A., Wickersham, M., Paulino, F., Peñaloza, H. F., . . . Prince, A. (2016). Necroptosis Promotes Staphylococcus aureus Clearance by Inhibiting Excessive Inflammatory Signaling. *Cell Rep, 16*(8), 2219-2230. doi:10.1016/j.celrep.2016.07.039

Klein, S. L., & Flanagan, K. L. (2016). Sex differences in immune responses. *Nat Rev Immunol, 16*(10), 626-638. doi:10.1038/nri.2016.90

Lawlor, K. E., Khan, N., Mildenhall, A., Gerlic, M., Croker, B. A., D'Cruz, A. A., . . . Vince, J. E. (2015). RIPK3 promotes cell death and NLRP3 inflammasome activation in the absence of MLKL. *Nat Commun, 6*, 6282. doi:10.1038/ncomms7282

Li, D., Ai, Y., Guo, J., Dong, B., Li, L., Cai, G., . . . Wang, X. (2020). Casein kinase 1G2 suppresses necroptosis-promoted testis aging by inhibiting receptor-interacting kinase 3. *Elife, 9*. doi:10.7554/eLife.61564

Li, D., Meng, L., Xu, T., Su, Y., Liu, X., Zhang, Z., & Wang, X. (2017). RIPK1-RIPK3-MLKL-dependent necrosis promotes the aging of mouse male reproductive system. *Elife, 6*. doi:10.7554/eLife.27692

Lin, J., Kumari, S., Kim, C., Van, T. M., Wachsmuth, L., Polykratis, A., & Pasparakis, M. (2016). RIPK1 counteracts ZBP1-mediated necroptosis to inhibit inflammation. *Nature, 540*(7631), 124-128. doi:10.1038/nature20558

Lin, Q. S., Chen, P., Wang, W. X., Lin, C. C., Zhou, Y., Yu, L. H., . . . Kang, D. Z. (2020). RIP1/RIP3/MLKL mediates dopaminergic neuron necroptosis in a mouse model of Parkinson disease. *Lab Invest, 100*(3), 503-511. doi:10.1038/s41374-019-0319-5

Lin, Y. H., Platt, M., Gilley, R. P., Brown, D., Dube, P. H., Yu, Y., & Gonzalez-Juarbe, N. (2021). Influenza Causes MLKL-Driven Cardiac Proteome Remodeling During Convalescence. *Circ Res*. doi:10.1161/circresaha.120.318511

Luedde, T., Kaplowitz, N., & Schwabe, R. F. (2014). Cell death and cell death responses in liver disease: mechanisms and clinical relevance. *Gastroenterology, 147*(4), 765-783.e764. doi:10.1053/j.gastro.2014.07.018

Miyata, T., Wu, X., Fan, X., Huang, E., Sanz-Garcia, C., Ross, C. K. C., . . . Nagy, L. E. (2021). Differential role of MLKL in alcohol-associated and non-alcohol-associated fatty liver diseases in mice and humans. *JCI Insight, 6*(4). doi:10.1172/jci.insight.140180

Moerke, C., Bleibaum, F., Kunzendorf, U., & Krautwald, S. (2019). Combined Knockout of RIPK3 and MLKL Reveals Unexpected Outcome in Tissue Injury and Inflammation. *Front Cell Dev Biol, 7*, 19. doi:10.3389/fcell.2019.00019

Moujalled, D., Gangatirkar, P., Kauppi, M., Corbin, J., Lebois, M., Murphy, J. M., . . . Josefsson, E. C. (2021). The necroptotic cell death pathway operates in megakaryocytes, but not in platelet synthesis. *Cell Death Dis, 12*(1), 133. doi:10.1038/s41419-021-03418-z

Mulay, S. R., Desai, J., Kumar, S. V., Eberhard, J. N., Thomasova, D., Romoli, S., . . . Anders, H. J. (2016). Cytotoxicity of crystals involves RIPK3-MLKL-mediated necroptosis. *Nat Commun, 7*, 10274. doi:10.1038/ncomms10274

Müller, T., Dewitz, C., Schmitz, J., Schröder, A. S., Bräsen, J. H., Stockwell, B. R., . . . Krautwald, S. (2017). Necroptosis and ferroptosis are alternative cell death pathways that operate in acute kidney failure. *Cell Mol Life Sci, 74*(19), 3631-3645. doi:10.1007/s00018-017-2547-4

Murphy, J. M., Czabotar, P. E., Hildebrand, J. M., Lucet, I. S., Zhang, J. G., Alvarez-Diaz, S., . . . Alexander, W. S. (2013). The pseudokinase MLKL mediates necroptosis via a molecular switch mechanism. *Immunity, 39*(3), 443-453. doi:10.1016/j.immuni.2013.06.018

Najjar, M., Saleh, D., Zelic, M., Nogusa, S., Shah, S., Tai, A., . . . Degterev, A. (2016). RIPK1 and RIPK3 Kinases Promote Cell-Death-Independent Inflammation by Toll-like Receptor 4. *Immunity, 45*(1), 46-59. doi:10.1016/j.immuni.2016.06.007

Nakazawa, D., Desai, J., Steiger, S., Müller, S., Devarapu, S. K., Mulay, S. R., . . . Anders, H. J. (2018). Activated platelets induce MLKL-driven neutrophil necroptosis and release of neutrophil extracellular traps in venous thrombosis. *Cell Death Discov, 4*, 6. doi:10.1038/s41420-018-0073-2

Newton, K., Dugger, D. L., Maltzman, A., Greve, J. M., Hedehus, M., Martin-McNulty, B., . . . Vucic, D. (2016). RIPK3 deficiency or catalytically inactive RIPK1 provides greater benefit than MLKL deficiency in mouse models of inflammation and tissue injury. *Cell Death Differ, 23*(9), 1565-1576. doi:10.1038/cdd.2016.46

Newton, K., Sun, X., & Dixit, V. M. (2004). Kinase RIP3 is dispensable for normal NF-kappa Bs, signaling by the B-cell and T-cell receptors, tumor necrosis factor receptor 1, and Toll-like receptors 2 and 4. *Mol Cell Biol, 24*(4), 1464-1469. doi:10.1128/mcb.24.4.1464-1469.2004

Ni, H. M., Chao, X., Kaseff, J., Deng, F., Wang, S., Shi, Y. H., . . . Jaeschke, H. (2019). Receptor-Interacting Serine/Threonine-Protein Kinase 3 (RIPK3)-Mixed Lineage Kinase Domain-Like Protein (MLKL)-Mediated Necroptosis Contributes to Ischemia-Reperfusion Injury of Steatotic Livers. *Am J Pathol, 189*(7), 1363-1374. doi:10.1016/j.ajpath.2019.03.010

Nogusa, S., Thapa, R. J., Dillon, C. P., Liedmann, S., Oguin, T. H., 3rd, Ingram, J. P., . . . Balachandran, S. (2016). RIPK3 Activates Parallel Pathways of MLKL-Driven Necroptosis and FADD-Mediated Apoptosis to Protect against Influenza A Virus. *Cell Host Microbe, 20*(1), 13-24. doi:10.1016/j.chom.2016.05.011

Pearson, J. S., & Murphy, J. M. (2017). Down the rabbit hole: Is necroptosis truly an innate response to infection? *Cell Microbiol, 19*(8). doi:10.1111/cmi.12750

Petrie, E. J., Sandow, J. J., Jacobsen, A. V., Smith, B. J., Griffin, M. D. W., Lucet, I. S., . . . Murphy, J. M. (2018). Conformational switching of the pseudokinase domain promotes human MLKL

tetramerization and cell death by necroptosis. *Nat Commun, 9*(1), 2422. doi:10.1038/s41467-018-04714-7

Petrie, E. J., Sandow, J. J., Lehmann, W. I. L., Liang, L. Y., Coursier, D., Young, S. N., . . . Murphy, J. M. (2019). Viral MLKL Homologs Subvert Necroptotic Cell Death by Sequestering Cellular RIPK3. *Cell Rep, 28*(13), 3309-3319.e3305. doi:10.1016/j.celrep.2019.08.055

Pierotti, C. L., Tanzer, M. C., Jacobsen, A. V., Hildebrand, J. M., Garnier, J. M., Sharma, P., . . . Lessene, G. (2020). Potent Inhibition of Necroptosis by Simultaneously Targeting Multiple Effectors of the Pathway. *ACS Chem Biol, 15*(10), 2702-2713. doi:10.1021/acschembio.0c00482

Polykratis, A., Martens, A., Eren, R. O., Shirasaki, Y., Yamagishi, M., Yamaguchi, Y., . . . Pasparakis, M. (2019). A20 prevents inflammasome-dependent arthritis by inhibiting macrophage necroptosis through its ZnF7 ubiquitin-binding domain. *Nat Cell Biol, 21*(6), 731-742. doi:10.1038/s41556-019-0324-3

Prevention, C. f. D. C. a. (2019). Pneumococcal Vaccination: Information for Healthcare Professionals. Retrieved from https://www.cdc.gov/vaccines/vpd/pneumo/hcp/index.html

Rasheed, A., Robichaud, S., Nguyen, M. A., Geoffrion, M., Wyatt, H., Cottee, M. L., . . . Rayner, K. J. (2020). Loss of MLKL (Mixed Lineage Kinase Domain-Like Protein) Decreases Necrotic Core but Increases Macrophage Lipid Accumulation in Atherosclerosis. *Arterioscler Thromb Vasc Biol, 40*(5), 1155-1167. doi:10.1161/atvbaha.119.313640

Rickard, J. A., Anderton, H., Etemadi, N., Nachbur, U., Darding, M., Peltzer, N., . . . Silke, J. (2014). TNFR1-dependent cell death drives inflammation in Sharpin-deficient mice. *Elife, 3*. doi:10.7554/eLife.03464

Riegler, A. N., Brissac, T., Gonzalez-Juarbe, N., & Orihuela, C. J. (2019). Necroptotic Cell Death Promotes Adaptive Immunity Against Colonizing Pneumococci. *Front Immunol, 10*, 615. doi:10.3389/fimmu.2019.00615

Robertson, S. J., Lemire, P., Maughan, H., Goethel, A., Turpin, W., Bedrani, L., . . . Philpott, D. J. (2019). Comparison of Co-housing and Littermate Methods for Microbiota Standardization in Mouse Models. *Cell Rep, 27*(6), 1910-1919.e1912. doi:10.1016/j.celrep.2019.04.023

Saeed, W. K., Jun, D. W., Jang, K., Oh, J. H., Chae, Y. J., Lee, J. S., . . . Kang, H. T. (2019). Decrease in fat de novo synthesis and chemokine ligand expression in non-alcoholic fatty liver disease caused by inhibition of mixed lineage kinase domain-like pseudokinase. *J Gastroenterol Hepatol, 34*(12), 2206-2218. doi:10.1111/jgh.14740

Sai, K., Parsons, C., House, J. S., Kathariou, S., & Ninomiya-Tsuji, J. (2019). Necroptosis mediators RIPK3 and MLKL suppress intracellular Listeria replication independently of host cell killing. *J Cell Biol, 218*(6), 1994-2005. doi:10.1083/jcb.201810014

Samson, A. L., Garnish, S. E., Hildebrand, J. M., & Murphy, J. M. (2021). Location, location, location: A compartmentalized view of TNF-induced necroptotic signaling. *Science Signaling, 14*(668), eabc6178. doi:10.1126/scisignal.abc6178

Schreiber, A., Rousselle, A., Becker, J. U., von Mässenhausen, A., Linkermann, A., & Kettritz, R. (2017). Necroptosis controls NET generation and mediates complement activation, endothelial damage, and autoimmune vasculitis. *Proc Natl Acad Sci U S A, 114*(45), E9618-e9625. doi:10.1073/pnas.1708247114

Schwarzer, R., Jiao, H., Wachsmuth, L., Tresch, A., & Pasparakis, M. (2020). FADD and Caspase-8 Regulate Gut Homeostasis and Inflammation by Controlling MLKL- and GSDMD-Mediated Death of Intestinal Epithelial Cells. *Immunity, 52*(6), 978-993.e976. doi:10.1016/j.immuni.2020.04.002

Shaw, A. C., Goldstein, D. R., & Montgomery, R. R. (2013). Age-dependent dysregulation of innate immunity. *Nat Rev Immunol, 13*(12), 875-887. doi:10.1038/nri3547

Sheridan, C. (2019). Death by inflammation: drug makers chase the master controller. *Nat Biotechnol, 37*(2), 111-113. doi:10.1038/s41587-019-0023-4

Shi, C., Kim, T., Steiger, S., Mulay, S. R., Klinkhammer, B. M., Bäuerle, T., . . . Anders, H. J. (2020). Crystal Clots as Therapeutic Target in Cholesterol Crystal Embolism. *Circ Res, 126*(8), e37-e52. doi:10.1161/circresaha.119.315625

Shindo, R., Ohmuraya, M., Komazawa-Sakon, S., Miyake, S., Deguchi, Y., Yamazaki, S., . . . Nakano, H. (2019). Necroptosis of Intestinal Epithelial Cells Induces Type 3 Innate Lymphoid Cell-Dependent Lethal Ileitis. *iScience, 15*, 536-551. doi:10.1016/j.isci.2019.05.011

Shubina, M., Tummers, B., Boyd, D. F., Zhang, T., Yin, C., Gautam, A., . . . Balachandran, S. (2020). Necroptosis restricts influenza A virus as a stand-alone cell death mechanism. *J Exp Med, 217*(11). doi:10.1084/jem.20191259

Siempos, II, Ma, K. C., Imamura, M., Baron, R. M., Fredenburgh, L. E., Huh, J. W., . . . Choi, A. M. (2018). RIPK3 mediates pathogenesis of experimental ventilator-induced lung injury. *JCI Insight, 3*(9). doi:10.1172/jci.insight.97102

Silke, J., & Hartland, E. L. (2013). Masters, marionettes and modulators: intersection of pathogen virulence factors and mammalian death receptor signaling. *Curr Opin Immunol, 25*(4), 436-440. doi:10.1016/j.coi.2013.05.011

Stutz, M. D., Ojaimi, S., Allison, C., Preston, S., Arandjelovic, P., Hildebrand, J. M., . . . Pellegrini, M. (2018). Necroptotic signaling is primed in Mycobacterium tuberculosis-infected macrophages, but its pathophysiological consequence in disease is restricted. *Cell Death Differ, 25*(5), 951-965. doi:10.1038/s41418-017-0031-1

Sun, L., Wang, H., Wang, Z., He, S., Chen, S., Liao, D., . . . Wang, X. (2012). Mixed lineage kinase domain-like protein mediates necrosis signaling downstream of RIP3 kinase. *Cell, 148*(1-2), 213-227. doi:10.1016/j.cell.2011.11.031

Sureshbabu, A., Patino, E., Ma, K. C., Laursen, K., Finkelsztein, E. J., Akchurin, O., . . . Choi, M. E. (2018). RIPK3 promotes sepsis-induced acute kidney injury via mitochondrial dysfunction. *JCI Insight, 3*(11). doi:10.1172/jci.insight.98411

Tanzer, M. C., Matti, I., Hildebrand, J. M., Young, S. N., Wardak, A., Tripaydonis, A., . . . Murphy, J. M. (2016). Evolutionary divergence of the necroptosis effector MLKL. *Cell Death Differ, 23*(7), 1185-1197. doi:10.1038/cdd.2015.169

Tanzer, M. C., Tripaydonis, A., Webb, A. I., Young, S. N., Varghese, L. N., Hall, C., . . . Murphy, J. M. (2015). Necroptosis signalling is tuned by phosphorylation of MLKL residues outside the pseudokinase domain activation loop. *Biochem J, 471*(2), 255-265. doi:10.1042/bj20150678

Tsurusaki, S., Tsuchiya, Y., Koumura, T., Nakasone, M., Sakamoto, T., Matsuoka, M., . . . Tanaka, M. (2019). Hepatic ferroptosis plays an important role as the trigger for initiating inflammation in nonalcoholic steatohepatitis. *Cell Death Dis, 10*(6), 449. doi:10.1038/s41419-019-1678-y

Tummers, B., Mari, L., Guy, C. S., Heckmann, B. L., Rodriguez, D. A., Rühl, S., . . . Green, D. R. (2020). Caspase-8-Dependent Inflammatory Responses Are Controlled by Its Adaptor, FADD, and Necroptosis. *Immunity, 52*(6), 994-1006.e1008. doi:10.1016/j.immuni.2020.04.010

Vanden Berghe, T., Kaiser, W. J., Bertrand, M. J., & Vandenabeele, P. (2015). Molecular crosstalk between apoptosis, necroptosis, and survival signaling. *Mol Cell Oncol, 2*(4), e975093. doi:10.4161/23723556.2014.975093

Wang, T., Perera, N. D., Chiam, M. D. F., Cuic, B., Wanniarachchillage, N., Tomas, D., . . . Turner, B. J. (2020). Necroptosis is dispensable for motor neuron degeneration in a mouse model of ALS. *Cell Death Differ, 27*(5), 1728-1739. doi:10.1038/s41418-019-0457-8

Webster, J. D., Kwon, Y. C., Park, S., Zhang, H., Corr, N., Ljumanovic, N., . . . Vucic, D. (2020). RIP1 kinase activity is critical for skin inflammation but not for viral propagation. *J Leukoc Biol, 107*(6), 941-952. doi:10.1002/jlb.3ma1219-398r

Weir, A., Hughes, S., Rashidi, M., Hildebrand, J. M., & Vince, J. E. (2021). Necroptotic movers and shakers: cell types, inflammatory drivers and diseases. *Curr Opin Immunol, 68*, 83-97. doi:10.1016/j.coi.2020.09.008

Wu, J., Huang, Z., Ren, J., Zhang, Z., He, P., Li, Y., . . . Han, J. (2013). Mlkl knockout mice demonstrate the indispensable role of Mlkl in necroptosis. *Cell Res, 23*(8), 994-1006. doi:10.1038/cr.2013.91

Wu, X., Poulsen, K. L., Sanz-Garcia, C., Huang, E., McMullen, M. R., Roychowdhury, S., . . . Nagy, L. E. (2020). MLKL-dependent signaling regulates autophagic flux in a murine model of non-alcohol-associated fatty liver and steatohepatitis. *J Hepatol, 73*(3), 616-627. doi:10.1016/j.jhep.2020.03.023

Xie, Y., Zhao, Y., Shi, L., Li, W., Chen, K., Li, M., . . . Xiao, H. (2020). Gut epithelial TSC1/mTOR controls RIPK3-dependent necroptosis in intestinal inflammation and cancer. *J Clin Invest, 130*(4), 2111-2128. doi:10.1172/jci133264

Xu, H., Du, X., Liu, G., Huang, S., Du, W., Zou, S., . . . Fu, X. (2019). The pseudokinase MLKL regulates hepatic insulin sensitivity independently of inflammation. *Mol Metab, 23*, 14-23. doi:10.1016/j.molmet.2019.02.003

Xu, Y., Ma, H., Shao, J., Wu, J., Zhou, L., Zhang, Z., . . . Han, J. (2015). A Role for Tubular Necroptosis in Cisplatin-Induced AKI. *J Am Soc Nephrol, 26*(11), 2647-2658. doi:10.1681/asn.2014080741

Yang, J., Zhao, Y., Zhang, L., Fan, H., Qi, C., Zhang, K., . . . Wu, S. (2018). RIPK3/MLKL-Mediated Neuronal Necroptosis Modulates the M1/M2 Polarization of Microglia/Macrophages in the Ischemic Cortex. *Cereb Cortex, 28*(7), 2622-2635. doi:10.1093/cercor/bhy089

Ying, Z., Pan, C., Shao, T., Liu, L., Li, L., Guo, D., . . . Wang, X. (2018). Mixed Lineage Kinase Domain-like Protein MLKL Breaks Down Myelin following Nerve Injury. *Mol Cell, 72*(3), 457-468.e455. doi:10.1016/j.molcel.2018.09.011

Yu, S. X., Chen, W., Liu, Z. Z., Zhou, F. H., Yan, S. Q., Hu, G. Q., . . . Yang, Y. J. (2018). Non-Hematopoietic MLKL Protects Against Salmonella Mucosal Infection by Enhancing Inflammasome Activation. *Front Immunol, 9*, 119. doi:10.3389/fimmu.2018.00119

Zhang, S., Su, Y., Ying, Z., Guo, D., Pan, C., Guo, J., . . . Wang, X. (2019). RIP1 kinase inhibitor halts the progression of an immune-induced demyelination disease at the stage of monocyte elevation. *Proc Natl Acad Sci U S A, 116*(12), 5675-5680. doi:10.1073/pnas.1819917116

Zhang, T., Yin, C., Boyd, D. F., Quarato, G., Ingram, J. P., Shubina, M., . . . Balachandran, S. (2020). Influenza Virus Z-RNAs Induce ZBP1-Mediated Necroptosis. *Cell, 180*(6), 1115-1129.e1113. doi:10.1016/j.cell.2020.02.050

Zhang, X., Fan, C., Zhang, H., Zhao, Q., Liu, Y., Xu, C., . . . Zhang, H. (2016). MLKL and FADD Are Critical for Suppressing Progressive Lymphoproliferative Disease and Activating the NLRP3 Inflammasome. *Cell Rep, 16*(12), 3247-3259. doi:10.1016/j.celrep.2016.06.103

Zhang, Y., Zhang, J., Yan, R., Tian, J., Zhang, Y., Zhang, J., . . . Dai, K. (2017). Receptor-interacting protein kinase 3 promotes platelet activation and thrombosis. *Proc Natl Acad Sci U S A, 114*(11), 2964-2969. doi:10.1073/pnas.1610963114

Zhao, J., Jitkaew, S., Cai, Z., Choksi, S., Li, Q., Luo, J., & Liu, Z. G. (2012). Mixed lineage kinase domain-like is a key receptor interacting protein 3 downstream component of TNF-induced necrosis. *Proc Natl Acad Sci U S A, 109*(14), 5322-5327. doi:10.1073/pnas.1200012109

Zhao, Q., Cheng, X., Guo, J., Bi, Y., Kuang, L., Ren, J., . . . Yu, X. (2021). MLKL inhibits intestinal tumorigenesis by suppressing STAT3 signaling pathway. *Int J Biol Sci, 17*(3), 869-881. doi:10.7150/ijbs.56152

Zhao, Q., Yu, X., Li, M., Liu, Y., Han, Y., Zhang, X., . . . Zhang, H. (2019). MLKL attenuates colon inflammation and colitis-tumorigenesis via suppression of inflammatory responses. *Cancer Lett, 459*, 100-111. doi:10.1016/j.canlet.2019.05.034

Zhou, S., Zhang, W., Cai, G., Ding, Y., Wei, C., Li, S., . . . Sun, L. (2020). Myofiber necroptosis promotes muscle stem cell proliferation via releasing Tenascin-C during regeneration. *Cell Res*. doi:10.1038/s41422-020-00393-6

 doi:10.20944/preprints202105.0053.v1